Bimaterial Microcantilevers as a Hybrid Sensing Platform**

By *Srikanth Singamaneni, Melburne C. LeMieux, Hans P. Lang, Christoph Gerber, Yee Lam, Stefan Zauscher, Panos G. Datskos, Nikolay V. Lavrik, Hao Jiang, Rajesh R. Naik, Timothy J. Bunning,* and *Vladimir V. Tsukruk**

50μm

Microcantilevers, one of the most common MEMS structures, have been introduced as a novel sensing paradigm nearly a decade ago. Ever since, the technology has emerged to find important applications in chemical, biological and physical sensing areas. Today the technology stands at the verge of providing the next generation of sophisticated sensors (such as artificial nose, artificial tongue) with extremely high sensitivity and miniature size. The article provides an overview of the modes of detection, theory behind the transduction mechanisms, materials employed as active layers, and some of the important applications. Emphasizing the material design aspects, the review underscores the most important findings, current trends, key challenges and future directions of the microcantilever based sensor technology.

[*]   Dr. T. J. Bunning, Prof. H. Jiang, Dr. R. R. Naik
        Materials and Manufacturing Directorate
        Air Force Research Laboratory
        Wright-Patterson Air Force Base
        OH-45433 (USA)
        E-mail: Timothy.Bunning@WPAFB.AF.MIL
        Prof. V. V. Tsukruk, S. Singamaneni, Dr. M. C. LeMieux
        School of Materials Science and Engineering,
        Georgia Institute of Technology
        Atlanta, GA-30332 (USA)
        E-mail: vladimir@mse.gatech.edu
        Prof. V. V. Tsukruk, S. Singamaneni
        School of Polymer, Textile and Fiber Engineering
        Georgia Institute of Technology
        Atlanta, GA-30332 (USA)
        Dr. M. C. LeMieux
        Chemical Engineering Department
        Stanford University
        Stanford, CA-94305 (USA)
        Prof. H. P. Lang, Prof. C. Gerber
        National Center of Competence in Research in Nanoscale Science
        Institute of Physics, University of Basel
        Klingelbergstrasse 82, 4056 Basel (Switzerland)
        Dr. Y. Lam, Prof. S. Zauscher
        Department of Mechanical Engineering and Materials Science
        Center for Biologically Inspired Materials and Materials Systems,
        Duke University
        Durham, NC (USA)

        Prof. P. G. Datskos, Dr. N. V. Lavrik
        Engineering Science and Technology Division
        Oak Ridge National Laboratory
        Oak Ridge, TN (USA)
        Prof. P. G. Datskos, Dr. N. V. Lavrik
        Department of Physics and Astronomy, University of Tennessee
        Knoxville, TN (USA)

1. Introduction

More so than ever, extreme detection with high selectivity of chemical and biological species and pathogens is becoming critical for our defense and civilian security.[1] Thus, a strong need exists for affordable sensor design that results in a single platform offering high potential functionality with simple signal transduction.[2,3] Soft materials are an excellent choice for this purpose not only because of ease and versatility of synthesis, batch-fabrication, and processability, but because their

Report Documentation Page			*Form Approved* *OMB No. 0704-0188*

Public reporting burden for the collection of information is estimated to average 1 hour per response, including the time for reviewing instructions, searching existing data sources, gathering and maintaining the data needed, and completing and reviewing the collection of information. Send comments regarding this burden estimate or any other aspect of this collection of information, including suggestions for reducing this burden, to Washington Headquarters Services, Directorate for Information Operations and Reports, 1215 Jefferson Davis Highway, Suite 1204, Arlington VA 22202-4302. Respondents should be aware that notwithstanding any other provision of law, no person shall be subject to a penalty for failing to comply with a collection of information if it does not display a currently valid OMB control number.

1. REPORT DATE **2008**	2. REPORT TYPE	3. DATES COVERED **00-00-2008 to 00-00-2008**

4. TITLE AND SUBTITLE	5a. CONTRACT NUMBER
Bimaterial Microcantilevers as a Hybrid Sensing Platform	5b. GRANT NUMBER
	5c. PROGRAM ELEMENT NUMBER
6. AUTHOR(S)	5d. PROJECT NUMBER
	5e. TASK NUMBER
	5f. WORK UNIT NUMBER

7. PERFORMING ORGANIZATION NAME(S) AND ADDRESS(ES) **Georgia Institute of Technology,School of Materials Science and Engineering,Atlanta,GA,30332**	8. PERFORMING ORGANIZATION REPORT NUMBER

9. SPONSORING/MONITORING AGENCY NAME(S) AND ADDRESS(ES)	10. SPONSOR/MONITOR'S ACRONYM(S)
	11. SPONSOR/MONITOR'S REPORT NUMBER(S)

12. DISTRIBUTION/AVAILABILITY STATEMENT **Approved for public release; distribution unlimited**

13. SUPPLEMENTARY NOTES

14. ABSTRACT

15. SUBJECT TERMS

16. SECURITY CLASSIFICATION OF:			17. LIMITATION OF ABSTRACT	18. NUMBER OF PAGES	19a. NAME OF RESPONSIBLE PERSON
a. REPORT **unclassified**	b. ABSTRACT **unclassified**	c. THIS PAGE **unclassified**	**Same as Report (SAR)**	**28**	

Standard Form 298 (Rev. 8-98)
Prescribed by ANSI Std Z39-18

high segmental mobility readily responds to an applied stimuli by exhibiting pronounced structural changes in the backbone, side chains, or end groups.[4–6] This molecular scale sensitivity can be engineered to respond to diverse stimuli because soft materials like Lego blocks offer a wealth of opportunities to design responsive structures triggered by various external stimuli.[7] These materials can possess unique topologies[8] leading to unique physical properties[9,10], or can be rendered for in-vivo sensing and drug-delivery.[11,12] Finally, the push to incorporate soft materials into next-generation sensors should

be considered a natural progression that is based on the principle of mimicking natural sensing structures in organisms that have had centuries to develop extreme sensing.[6,13] Whereas semiconductors and metal oxides have been the traditional *active sensing material*s in microelectromechanical systems (MEMS), soft matter-inclusive sensors bring a desirable diversity in signal transduction principles, tailorability, and multifunctionality that the traditional materials cannot offer.[14] On the other hand, inorganic materials (such as silicon) are well established in microdevices, and this foundation

Timothy J. Bunning is a Principal Materials Research Engineer in the Materials and Manufacturing Directorate, part of the Air Force Research Laboratory. Dr. Bunning received a Ph.D. from the University of Connecticut in Chemical Engineering. His current research interests are centered on the optical, electro-optical, and photo-optical performance of structured polymeric and liquid crystalline materials. Central research areas include the development of 1-, 2-, and 3D switchable polymeric diffractive structures using complex holographic photopolymerization techniques, development of novel polymeric thin films using plasma enhanced chemical vapor deposition, and phototunable materials. He is a Fellow of the American Physical Society, and Society for Optical Engineering and received the American Physical Society's Dillon Medal. He research credentials include 230+ technical publications (150+ peer-reviewed), 420 presentations (140+ invited presentations, 12 patents, and several book chapters and edited books.

Vladimir V. Tsukruk received his M.S. degree in Physics from the National University of Ukraine, Ph.D and DSc in Chemistry from the National Academy of Sciences of Ukraine (Yu. Lipatov), and was a postdoc with J. Wendorff (U. Marburg) and D. Reneker (U. Akron). Currently, he holds a joint appointment as a Professor at the School of Materials Science and Engineering and School of Polymer, Fiber, and Textile Engineering, Georgia Institute of Technology. He has co-authored 250+ refereed articles, 18 invited reviews, one book, co-edited three volumes, and holds four patents. His research activities in the fields of surfaces/interfaces, molecular assembly, nano- and bioinspired materials are honored by the NSF Special Creativity Award (2006), AFOSR Faculty Research Fellowship (1995), NSF RIA Young Investigator Award (1994), Humboldt Fellowship (1990), Best Young Investigator Research Prize in Ukraine (1985), among others. He serves on the editorial advisory boards of Polymer and Curr. Chem. Biology.

Srikanth Singamaneni received his M.S. degree (2004) in Electrical Engineering from Western Michigan University and currently pursuing his Ph.D. in Polymer Materials Science and Engineering at Georgia Institute of Technology. He has co-authored more than 25 refereed articles in archival journals and made presentations at National Conferences. He was a recipient of the Best Poster Award at Materials Research Society National Meeting, Spring 2007. His current scientific interests include the fabrication of organic and inorganic nanostructured materials for advanced physical and chemical sensors, and interaction of electromagnetic radiation with metal nanostructures.

is not likely to change anytime soon. Thus, hybrid structures, which consist of these two very diverse components, should be considered as an attractive design paradigm to advance sensor science and technology.

1.1. Responsive Soft Materials

Adaptive and responsive soft materials with tunable properties that are readily controlled by environmental conditions (temperature, ionic strength, pH, electrical field) represent a critical, and now well-matured field in nanotechnology. These materials are considered outstanding candidates for assembling "smart" or "intelligent" active structures, and thus are instrumental for sensor designs which require an agile response to minute disturbances.[7] Significant efforts have been made to design, prepare, characterize, and understand the structure-properties relationships of such stimuli responsive materials (SRM) in a bulk state or thin films either as ultrathin surface layers, or in free-standing state.[4,15–17] SRMs are defined as materials that undergo relatively large, reversible and *abrupt* physical, chemical, or structural changes in response to small external changes in the local environmental conditions.[18] It has been demonstrated that the reorganization of these materials on a molecular scale translates to dramatic changes in bulk and surface properties, thus, creating switchable or responsive materials with controlled wettability, mechanical response, heterogeneity, charge, adhesion, and chemical functionality, all of which can be potentially exploited for both sensing and microactuation.[19,20]

Among materials and structures widely used as responsive media are self-assembled monolayers (SAMs) from alkylsilanes and alkylthoils, Langmuir–Blodgett (LB) films from various amphiphilic molecules, homo- and copolymers with different chain architectures, grafted-to and -from polymer brush layers, polymer layers filled with inorganic and carbon nanoparticles and tubes, biological molecules with selective binding abilities, and molecules with "clickable" molecular shape.[4,7,8,16,21] The ability of these materials to act as the responsive media is directly related to the ability of intra- or intermolecular reorganization controlled/triggered by subtle changes in weak interactions with external stimuli and analytes. Two prominent examples are dramatic changes in surface tension/energy of functionalized SAMs upon adsorption of even few molecules and collapse/swelling of polymer brushes after treatment with bad or good solvents (see discussion below).[19,22]

SAMs remain very popular responsive materials due to relatively easy formation of these dense, robust, and uniform monolayers with readily controllable surface functionality. This way, surface properties can be controlled ranging from highly hydrophobic state for methyl- and fluoro-terminated SAMs to highly hydrophilic state of carboxy- and hydroxyl-terminated SAMs or highly reactive functionality of epoxy- and amino-terminated SAMs.[22–25] Their ability to selectively bind to specific analyte molecules from solution or gas phase

followed by dramatic changes in surface energy, intermolecular ordering, or overall monolayer mass is widely recognized as a means to detect these binding effects.

Numerous classes of polymers and structures such as cross-linked and reversible hydrogels, brush macromolecules, micelles and polymer/biopolymer conjugates have been employed for various applications including sensing, actuation, delivery of therapeutics, tissue engineering, and bioseperations.[4,5,18,26,27] For instance, hydrogels are three-dimensional (3D) network of polymer chains, chemically or physically linked with each other, partially solvated by water molecules. Their unique structure enables them to exhibit large reversible swelling in aqueous environment making them excellent responsive materials. Stimuli-responsive hydrogels could be reversibly transformed by environmental stimuli, exhibiting abrupt sol–gel transition with dramatic change of volume and properties.[28,29] On the other hand, poly(*N*-isopropylacrylamide) (PNIPAM) is probably the most studied synthetic responsive polymer which undergoes an LCST phase transition at physiologically relevant 32 °C changing from a hydrophilic state (below LCST) to a hydrophobic state (above LCST). Moreover, the phase transition temperature of the PNIPAM can be tuned by incorporation of co-monomer units into the homopolymer.[30,31] Thin polymer films and patterned surface layers from PNIPAM-based materials and some other block-copolymers show switchable adhesive and mechanical properties.[32–34]

For amphiphilic block copolymers, hydrophobic effect causes different blocks to aggregate and form micelles in aqueous medium. There are several examples demonstrating the structural changes in these polymer micelles under varying pH and temperature.[35,36] For example, poly(alkene oxides) combined with poly(styrene) forms permanent nanoparticles due to the self-organization of this AB diblock copolymer. Peculiar stimuli-sensitive surface behavior was demonstrated for single molecules, gradient films, and monolayer films of dendritic copolymers, star block copolymers, ABA tri-block copolymers.[37–41]

Yet another important class of materials, which have been extensively investigated for responsive surfaces are the so called *polymer brushes*.[42–44] In its simplest form, polymer brush is comprised of grafted polymer chains extending away from the substrate so that the end-to-end distance in a good solvent is larger than unperturbed dimensions. Similar to any other responsive system, external stimuli cause conformational reorganization (collapse-swelling) resulting in polymer brushes to exhibit large and reversible changes in the thickness, adhesion, wettability, or affinity to a particular analyte depending on the design of the brush layers (binary brushes, Y-shaped, grafted to or grafted from).[45–52]

Ultrathin films of homopolymers and composite structures have been applied as responsive medium for various applications. For example, sensors employing thin films of polyaniline have been very effective for aqueous media.[53] These films possess excellent stability and show rapid reversible color change upon pH change due to varying degrees of protona-

tion of the imine nitrogen atoms.[54,55] Prospective applications include sensors in microfluidic systems such as pH sensitive gates, oxidoreduction sensitive gates, and photo-controlled chemical gates to regulate flow through membranes.[56–59] Humidity sensors based on polymer thin films have been developed that work on the principle that ion conducting polymer systems undergo a variation of the electrical conductivity with a variable water vapor content.[60]

There are numerous examples of thermal, gas, chemical, and biosensors based on the exploitation of specific interactions within soft materials.[6] For example, polyacetylene experiences a change in conductivity of eleven orders of magnitude when exposed to iodine vapor.[61] Other heterocyclic polymers, which retain the π-system, were later developed, and include polyfurans, polythiophenes, and polypyrroles.[62,63] The fundamental responsive mechanism in these polymers allowing strong changes in electrical and optical properties on exposure to a host of chemical analytes is the extended π-conjugation easily disturbed by molecular interactions. These property changes can be observed at room temperature when they are exposed to trace amount of analytes, which make them ideal candidates for materials in gas sensors.[64]

1.2. Responsive Hybrid Structures

While soft materials are the best *active sensing* materials they do not always provide the best platform for microfabrication and miniaturization.[65] On the other hand, whereas semiconductors and metal oxides are the traditional *active materials* in sensing applications, they are not always versatile enough to provide multifunctional behavior. Conversely, inorganic materials are well established in microdevices and microfabrication. Incorporation of SRM into sensory systems brings a desirable diversity in signal transduction principles, tailorability, and multifunctionality that these traditional materials cannot offer.[14] A combination of metal nanoparticles with responsive polymer shells, surface brushes, or multilayered layer-by-layer films was demonstrated to be prospective hybrid structures for sensing applications.[66–75] Thus, hybrid structures, which consist of these two very diverse material components, should be considered as a strong design paradigm for responsive materials and structures.

Although most of soft-material based sensors exhibit performance, in terms of sensitivity, that surpasses that of sensors made of traditional inorganic materials, they have several drawbacks, currently limiting their usefulness for demanding sensing applications. The primary negative aspect of most of soft-matter-based sensors is the thickness of the sensing layer, which must be typically on the order of several micrometers to provide sufficient sensi-

tivity. This exceeding dimension limits the incorporation of these sensing layers into micro and nano-scale sensors. Even the so-called "ultrathin" sensors still usually have 300+ nm thick films in the best (thinnest) cases.[76,77] Moreover, such coatings are commonly applied to electrodes[77] by a photo-patterning process that involves complicated photolithography.[78]

Besides the size, construction, and robustness issues, the traditional sensors are usually engineered to sense only one specific analyte or employ only one detection mode (either pH or humidity), and it is unclear whether they can be fabricated to be more diverse. Thus, these designs are typically "niche" sensors and are only useful if one specific type of response must be determined. However, in real-life applications with a number of external stimuli to be monitored, this is not practical. For example, weapons or threat sensing applications require a single sensor that can reliably sense several different gases and chemicals simultaneously and provide selective response. It is useless if a sensor reads "all clear" to VX nerve gas because it does not sense the thiolate group, but the user drops dead to mustard gas because the sulfonium salt that attacks the skin could not be detected. Clearly, sensors must be designed and fabricated to be as dynamic as possible, and capable of responding to diverse environmental stimuli.

To design, fabricate, and implement SRMs into hybrid organic-inorganic sensors, several steps must be undertaken. These efforts can be split into three distinct phases as outlined in a Design Approach Pyramid depicted in Figure 1 with major aspects to be discussed in this review for a class of cantilever-based sensors. We believe that the combination of SRMs and microfabricated, inorganic platform such as microcantilevers (MC) is the most promising way.

In this review, a particular emphasis is given to the design and selection of responsive materials which are important for
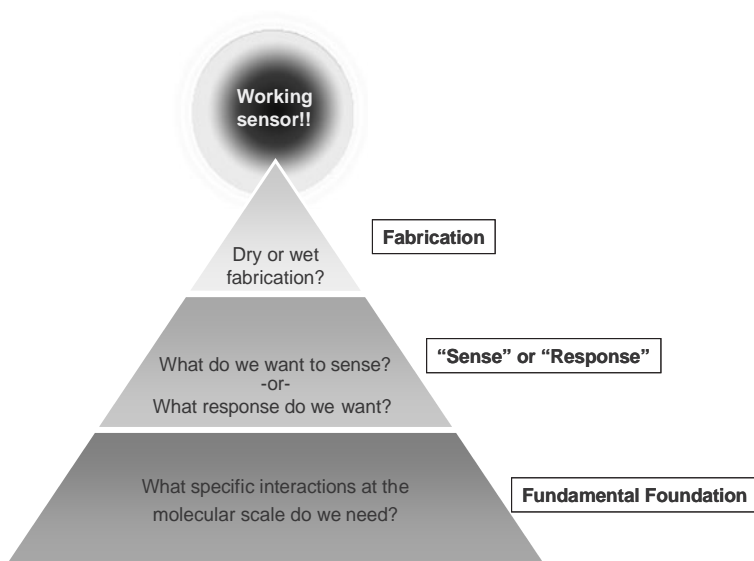

Figure 1. Diagram showing the "Approach Pyramid" that depicts the considerations involved in producing a working sensing element.

several key attributes critical for the ultimate performance of bimaterial, hybrid MC sensors. We review the materials selection of the MCs themselves, the sensitive coatings employed, and their specific design for important applications in chemical and biological sensing. We discuss the key issues, which need to be addressed in the future before the technology can provide the next generation of the miniaturized sensors for applications spanning the life sciences, industrial processes, and antiterrorist activities. A short overview of novel related microstructures such as arrays of MCs, microtuning fork structures, and nanocantilevers is presented as well.

The selection of this topic for a comprehensive review is justified not just by the fact that the authors stay active in this field for a long time but an overall sharp upward recent trend in research activities in this field brought by modern realities and a changing funding focus. In fact, in just over a decade, MC-based sensing technology has witnessed a rapid progress due to the significant attention by a multidiscipilnary scientific community, evident from the steady increase in the number of publications in the last 10 years from a trivial level of a few occasional reports in the beginning of 90s to more than 200 peer-reviewed papers annualy today (Fig. 2). In the last decade, MC-based sensors have proved to become a versatile tranduction platform for various physical, chemical, and bio-
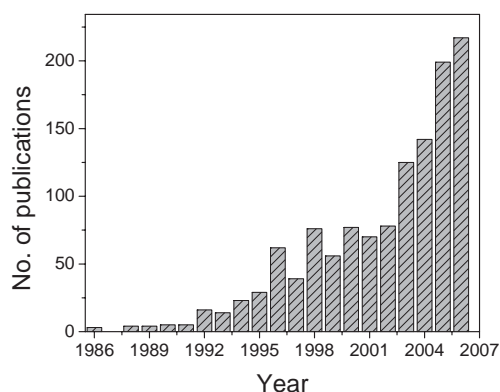

Figure 2. Plot showing the number of annual peer reviewed publications as obtained from SCI FINDER search with a key "cantilever sensor".

logical sensors. The complementary signals obtained from MCs in the form of static deflection, resonance frequency shift, and change in the Q-factor enable unambiguos detection of trace amounts of organic vapors, explosives, chemical and biological warfare agents with extreme accuracy. Apparently, such a spur of activities and results needs to be systemized and evaluated.

2. Trends in Microcantilever Sensor Research

In spite of the active developments of various transduction mechanisms, which include but are not limited to mechanical, electrical, optical, acoustic, electro-optical, and electrochemi-

cal methods, the field of sensor design and engineering has witnessed a continued search for the ideal signal transduction mechanism to maximize the transduction efficiency. While atomic force microscopy (AFM), introduced in the mid 80s, is an important milestone in nanoscience and technology, it also fueled a revived interest in microfabrication, and a plethora of applications of micromechanical structures.[79] AFM has long relied on MCs as transducers for its numerous imaging modes[80,81] including topographical, electric potential, magnetic, and force imaging. As a natural succession to their application as force transducers in AFM, MCs were selected as a new platform for transduction in sensing technology more than a decade ago.[82] Ever since, the technology has emerged to find important applications in chemical, biological, and thermal sensing.

There are a number of cantilever configurations (e.g., with and without intrinsic stress, silicon vs. polymer, "diving boards" vs. V-shaped) designed for various applications (thermal sensing, IR sensing, chemical sensing, or biosensing). Within each sensing paradigm, there are different implementation principles – e.g., for chemical sensing, one can sense induced stress, weight change, reflectance change, and so on. The change of stress can be measured by piezoresistive elements, piezoelectric elements, MOS transistor, or light beam deflections, to name a few. The microscopic levers can be fabricated into various geometries with specific coatings using a vast range of semiconducting and metallic materials to optimize stiffness (kb/T noise), conductivity, reflectance, and Q factor. It is a huge challenge to cover existing accomplishments and future trends in a whole sub-field of microcantilever-based sensing. However, detailed discussion of the full range of possible cantilever designs is not the subject of this review. We focus mainly on materials aspect of their design which is critical for ultimate sensing applications.

To provide sensing ability to microcantilever beams, their top and bottom surfaces must be coated in a chemically well-defined way to provide a functional surface capable of reacting with the target molecules and a passivated surface that will not significantly react with the target molecules thus creating differential stresses. In this section, we briefly introduce the MC based transduction principles along with each operation mode and detection methods of MC based sensors (Fig. 3). Chemical reaction and deflagration methods of detection are also presented here as practically important approaches.

2.1. Basic Modes of Operation and Detection

There are two basic modes of operation of MC-based sensors namely, static (physical deflection of the MC) and dynamic (change in resonance frequency/phase) as well as several ways to initiate cantilever reaction such as, e.g., heat (deflection due to differential thermal expansion) or chemical reaction (Fig. 3). In another example, adsorption of molecules onto the surface of the MC causes a bending due to increasing interfacial stress. Each mode differs from other in terms of the
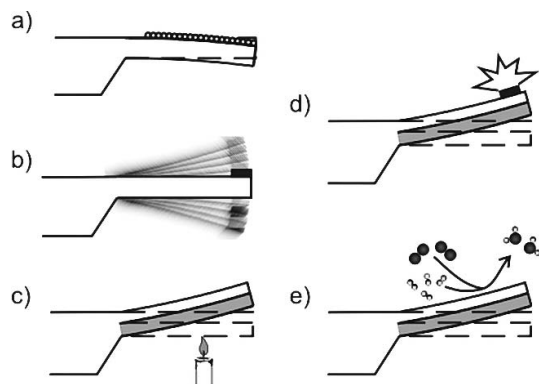
Figure 3. Schematic representation of various modes of operation of MCs: a) Surface stress due to absorption of molecules causing static deflection; b) Dynamic resonance frequency shift mode due to change in effective mass; c) Heat sensing mode due to differential thermal expansion; d) Deflagration of explosive on the heated MC surface; e) catalytic reaction on the cantilever surface.

Figure 4. Schematic representation of MC deflecting in static mode under surface stress (a); MC oscillating at fundamental frequency f_o (b); and viscous damping for under-liquid operation (c) along with corresponding parameters.

principle of transduction, functionalization, and detection mechanisms. Here we briefly introduce major modes of operation and highlight the design considerations specific to each mode.

2.1.1. Static Deflection Mode

The asymmetry of a functionalized top surface and a passivated bottom surface is especially important for the static deflection mode. The MC flexural behavior is controlled by the spring constant k of the cantilever, which is defined by material properties and MC geometrical dimensions. For a rectangular microcantilever of length l, thickness t, and width w, the spring constant k is calculated as follows:

$$k = \frac{Ewt^3}{4l^3} \qquad (1)$$

where E is Young's modulus ($E_{Si} = 1.3 \times 10^{11}$ N m^{-2} for Si(100)). Typical spring constants for common MCs of several hundred micrometers length and a thickness below 1 μm fall in the range of 0.001 to 0.1 N m^{-1}. Actual spring constants can be calculated and measured for various complicated shapes and compositions by using a range of theoretical and experimental approaches as has been discussed elsewhere.[83,84]

Assuming that uniform surface stress, $\Delta\sigma$, over the whole area of the cantilever is the cause for bending, the shape of the bent microcantilever can be approximated as part of a circle with radius R given by Stoney's equation[85,86]

$$\frac{1}{R} = \frac{6(1-v)}{Et^2}\Delta\sigma \qquad (2)$$

where v is the Poisson's ratio ($v_{Si} = 0.24$). For a given deflection, the surface stress change (schematically represented in Fig. 4a) can be derived by using Equation 2, which is however valid only for a surface layer much thinner than the beam
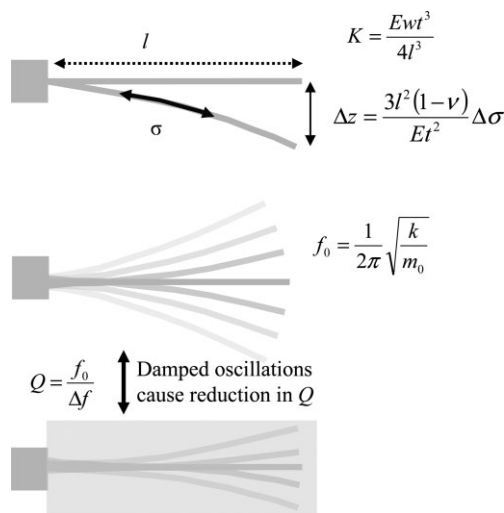
itself (< 20 %).[85] There have been several attempts to modify Stoney's equation for thicker layers, the accuracy of which have been reviewed in a recent article.[87]

Static deflection operation (constant deflection at a given constant stress) is possible in various environments such as vacuum, ambient, and fluidic. In a gaseous environment, molecules adsorb on the functionalized sensing surface and form a molecular layer, provided there is affinity for the molecules to adhere to the surface. Static-mode operation in liquids, however, usually requires rather specific sensing layers, based on molecular recognition, such as DNA hybridization or antigen-antibody recognition as will be discussed below.

Polymer sensing layers frequently show a partial selectivity, because molecules from the environment diffuse into the polymer layer at different rates, mainly depending on the size and solubility of the molecules in the polymer layer. By selecting polymers expressing a wide range of hydrophilic/hydrophobic ligands, the chemical affinity of the surface can be manipulated to bind various molecules through intermolecular forces such as ionic bonds, hydrogen bonds and van der Waals forces.

2.1.2. Dynamic Resonance Frequency Shift Mode

By oscillating a MC at its eigenfrequency (f_0, the resonance frequency of an oscillating microcantilever is constant if its elastic properties remain unchanged during the molecule adsorption/desorption process and damping effects are negligible), information of adsorption or desorption of mass can be obtained under the prerequisite that the molecules on the surface might be in a dynamic equilibrium with molecules from the environment.

The corresponding mass changes can be determined by tracking the change in eigen frequency (Δf_0) of the microcan-

ADVANCED MATERIALS

tilever during mass adsorption or desorption (as shown schematically in Fig. 4b). In this dynamic mode, MC is used as a microbalance, with added mass on the surface causing the resonance frequency to shift to a lower value. The mass change on a rectangular cantilever during molecular adsorption is related to the resonance frequency shift according to[88]

$$\Delta m = \frac{k}{4\pi^2 n} \times \left(\frac{1}{f_0^2} - \frac{1}{f_1^2}\right) \tag{3}$$

where n is a geometric parameter and equals 0.24 for rectangular cantilevers and f_1 the eigenfrequency after the mass change.

Mass-change determination can be combined with variable but controlled temperature to facilitate "micromechanical thermogravimetry".[89] In the mass-balance mode, the sample under investigation is mounted at the apex of the cantilever, however, its mass should not exceed several hundred nanograms. In the case of adsorption or desorption (or decomposition processes), mass changes in the low picogram range can then be detected in real time.

Dynamic mode works efficiently in the gas phase where the quality factor remains virtually unchanged as compared to vacuum (the resonance frequency shifts by a few percents). However, in liquid environment, this approach suffers from substantial damping of the cantilever oscillation due to high viscosity of the surrounding medium increasing drag forces significantly (by several orders of magnitude). This damping results in a low quality factor $Q = \frac{f_0}{\Delta f}$., where Δf is the full width half maximum of the frequency spectrum. The dramatic drop in the quality factor is usually observed from the typical range of 100–1000 in air to values below 50. Under these conditions, the resonance frequency shift is difficult to track with high resolution and thus the overall sensitivity decreases dramatically. While in air a frequency resolution of below 1 Hz is easily achieved for common cantilevers, resolution values of only about 20 Hz is considered very good for measurements in liquid environment. Moreover, in the case of damping or changes of the elastic properties of the cantilever during the experiment, e.g., stiffening or softening by adsorption of a molecule layer, the measured resonance frequency will not be exactly the same as the eigenfrequency, and the mass derived from the frequency shift will be inaccurate. Dynamic operation in large damping environment is described in detail in Ref. [90].

A novel design for interrogation of solution eliminating these difficulties has been very recently reported by Burg et al.[91] The authors suggested the fabrication of the MCs with microfluidic channels embedded into the cantilever as shown in Figure 5a. The fluid continuously flowing through the channel to deliver the analyte species causes a change in the resonant frequency of the suspended microchannel due to binding of the analyte to the complementary species without compromising on the cantilever performance (Fig. 5b). A transient flow of the particle through the channel results in temporal
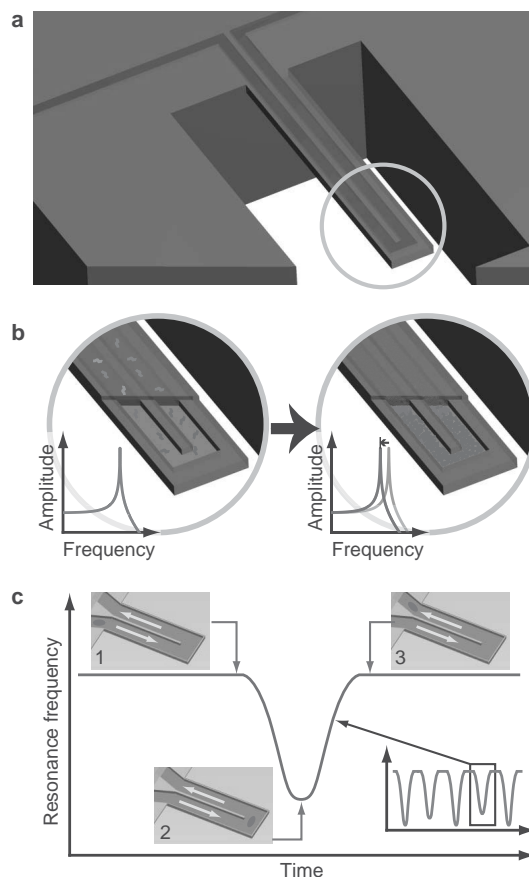

Figure 5. Schematic representation of the suspended microfluidic resonator structure (a) and the resonance response of the structure (b) for analyte binding to the complementary species and the transient resonance shift for the particles traversing the channel (c). Reproduced with permission from [91]. Copyright 2007 Nature Publishing Group.

dips in the resonance frequency (Fig. 5c) depending on the position of the particles along the channel. An excellent quality factor of 15000 was reported for a microresonator channel filled with water or air and the ability to detect single biomolecules and nanoparticles in fluid with a mass resolution reaching 300 attograms was demonstrated.[91] It is important to note that the typical quality factor for a MC submerged in liquid is more than two orders of magnitude smaller. This new design paradigm has the potential to significantly improve the applications of MCs for fluidic environment.

2.1.3. Heat Sensing Behavior

Bimaterial MCs comprised of two layers exhibit bending with change in temperature due to thermal expansion differences (Fig. 6). This very well-known phenomenon is frequently referred to as the "bimetallic effect" and corresponding structures are called bimorphs.[92,93] In reference to the MC-based sensors, this mode of operation is frequently referred to as 'heat mode'.[82] Due to the differential thermal expansion, silicon nitride cantilevers, for example, with a thin
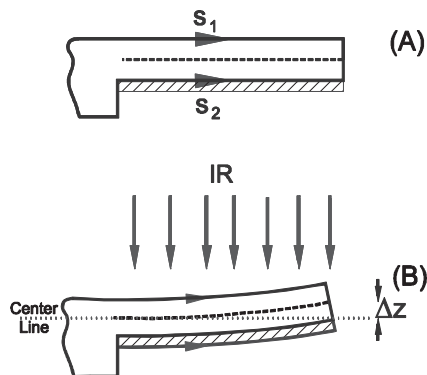
ADVANCED MATERIALS

Figure 6. Schematic representation of the bimaterial structure applied for IR imaging: a) bimaterial MC in rest; b) static deflection of the MC due to the differential thermal expansion.

gold film on one side undergo measurable bending in response to extremely small temperature changes due to the differential stress in the cantilever generated by dissimilar thermal expansion of the silicon nitride cantilever and the gold coating (Fig. 6).[15] Heat change can be either caused by external influences, such as change in environmental temperature (thermal detection), or occuring directly on the surface by catalytic reaction, or initiated by the thermal material properties of a sample attached to the apex of the cantilever (micromechanical calorimetry).

The steady state deflection of the tip of a bimaterial cantilever in response to a temperature change, ΔT, is given by[93]

$$\Delta z = \frac{3l_b^2}{t_1 + t_2}\left[\frac{\left(1 + \frac{t_1}{t_2}\right)}{3 + \left(1 + \frac{t_1}{t_2}\right)^2 + \left(1 + \frac{t_1}{t_2}\frac{E_1}{E_2}\right)\left(\frac{t_1^2}{t_2^2} + \frac{t_2}{t_1}\frac{E_2}{E_1}\right)}\right](a_1 - a_2)\Delta T \quad (4)$$

where l_b is the bimaterial microcantilever length, t_1 and t_2 are the thickness of the coating and the microcantilever substrate, a_1 and a_2 are the thermal expansion coefficients of the coating and microcantilever, and E_1 and E_2 are the corresponding Young's moduli. As shown in Figure 6, Δz refers to the vertical deflection of the centerline of the microcantilever, at its outmost (right) end.

It can be concluded from Equation 4 that the Δz linearly depends upon difference in thermal expansion coefficients and temperature gradient. The deflection also can be maximized by designing MCs with proper geometry in addition to selecting appropriate bimaterial layers. Although the thickness of each layer as well as the overall length of the cantilever have a dramatic effect on the displacement magnitude, optimi-

zation of the cantilever design can not be achieved based on the condition of the maximum displacement alone. For example, the amplitude of cantilever deflection increases as the square of the bimaterial length, l_b. However, as the cantilever length increases so does the thermal noise which limits the achievable resolution. However, the best sensitivity of the cantilever heat mode is orders of magnitude higher than that of traditional thermal methods performed on milligram samples, as it only requires nanogram amounts of sample and achieves nanojoules[94] to picojoules[95,96] sensitivity.

2.2. Transduction Mechanisms

A number of different phenomena acting concurrently might cause MC static and dynamic response. For instance, as was discussed above, differential thermal expansion of the cantilever substrate and coating layer results in the bending of the bimaterial cantilever which can reach 60 nm per degree (Fig. 7). However, the differential thermal expansion can be caused by other reasons such as radiation induced background heating or an exothermic reaction caused by analyte adsorption. Alternately, the changes of the differential surface energy can be caused by preferential adsorption of the analyte due to mass change without any reaction or the surface tension stress due to the liquid phase on one side of the cantilever (capillary phenomenon).

Here, we will briefly discuss the role and level of contributions in the cantilever bending of different factors. Figure 7 summarizes the most common transduction mechanisms with typical attributes such as the stress and deflection of the MC or the resonance frequency shift. The estimation of the linear stresses developed and corresponding typical cantilever deflections have been estimated by using the Stoney's equation and literature data available.
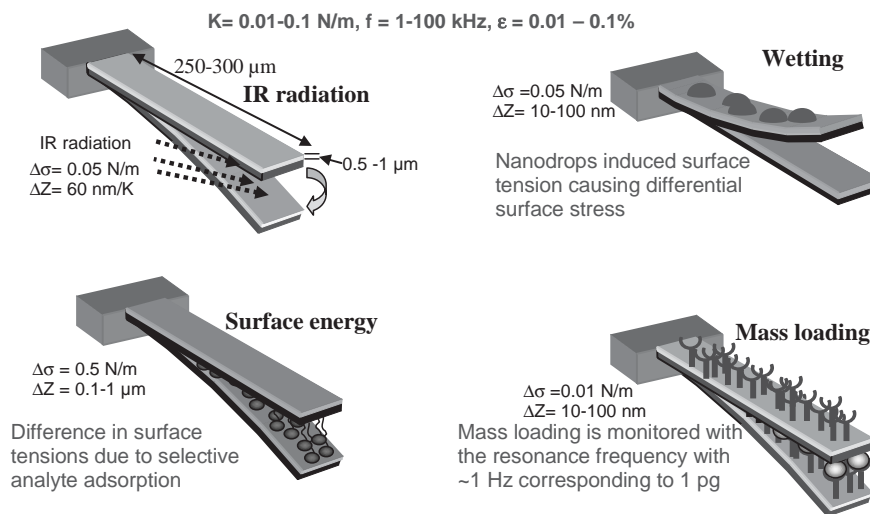

Figure 7. Schematic representation of the transduction mechanisms of MC based sensors with the typical range of the surface stress and the deflection achieved in each case for typical MC dimensions.

ADVANCED MATERIALS

In the capillary phenomenon, the liquid droplets adsorbed on the surface of the cantilever apply normal forces on the cantilever due to the vertical component of the surface energy of liquid-vapor interface. It has been recently experimentally demonstrated that the vertical component ($\gamma_{LV} \sin\check{\iota}$) of the surface energy, which is neglected for immovable surfaces in the Young's equation, can cause significant deflection of freely suspended structures but, generally, the static deflection caused by this phenomenon does not exceed 100 nm.[97]

The differential surface stress due to preferential adsorption of the analyte is the primary transduction mechanism for MCs functionalized with SAMs and metals where coatings have special affinity to the analyte molecules while the other surface remains largely insensitive to them. Differential stress can be as high as 0.5 N m^{-1} resulting in large static deflections approaching 1000 nm, both high values far exceeding any other contributions (Fig. 7). Moreover, dimensional changes in the sensitive materials (e.g., polymer layers) due to the sorption of the analyte molecules termed as swelling or de-swelling might result in even larger interfacial stress (as high as few MPa in some cases discussed below) in the bimaterial structure causing the bending of the entire structure by many micrometers clearly overshadowing other contributions.

Adsorption and desorption of the analyte on the surface and bulk of the functional coating result in change in the effective mass. The overall stress developed is not very high (below 0.01 N m^{-1}) and the deflection is modest (around 10 nm in most cases) and are difficult to detect (Fig. 7). Biomolecular interactions (DNA hybridization, protein conformation changes, antibody-antigen interactions) also cause a shift in resonance frequency or cantilever deflection due to differential surface stress.[98] This deflection originates from osmotic pressure when biomolecules bind closely packed on one surface of the lever. Practical deflection measurements thus typically rely on high surface density of receptor molecules and close packing of bound analyte rather than on just added mass effect. The resonance frequency of the microcantilever decreases as mass is bound to the surface with typical sensitivity approaching 1 pg/Hz. Changes in resonance frequency are typically concurrent with deflection of the cantilever.

2.3. Methods of Detection

Numerous methods have been developed for the monitoring the MC deflection in the context of their application as force transducers. The detection schemes employed can be classified broadly as optical (optical lever and interferometry) and electrical schemes (piezoresisitve, piezoelectric, capacitance, electron tunneling). The optical lever technique in which light is reflected from the back of the MC onto a position sensitive photodetector is similar to the readout scheme widely used in commercial AFM systems.[99] The deflection of the cantilever is thus translated in photodiode output voltage which, with proper calibration, can be converted into actual z-deflection. This technique, which offers a detection limit better than 1 Å and is mainly limited by thermal vibrations, was successfully adapted for the detection of static and dynamic signals in MC based sensors. This method has been extended to cantilever arrays using multiple lasers.[100] Light from eight individual light sources can be coupled into an array of multimode fibers and guided onto the sensor array. Reflected light is directed to a position-sensitive detector (PSD) and the photocurrents are converted into voltages. In recent study, the eight light sources were switched on and off individually and sequentially detected by time-multiplexing.[101]

Apart from the disadvantages such as requirement of precise alignment, low opacity and low turbidity medium of operation, the primary drawback of this approach is the limited bandwidth which makes it extremely difficult to extend it to arrays of cantilevers and nanomechanical resonant structures. In contrast, optical interferometry offers higher bandwidth measurement and has been introduced as a MEMS-based technique which shows a great promise for the readout approach for large MC arrays.[102,103]

Piezoresistivity of a material (e.g., doped silicon) under external strain has been translated to monitor the deflection of the MCs.[104–106] Piezoresisitive detection method obviates the need for a complex alignment procedure which is often a serious problem in optical based detection methods. It is also important to note that piezoresistance method facilitates the measurement of huge deflections while the optical detection method is limited to a smaller range (typically few micrometers). However, in addition to the lower resolution (typically 0.5 to 1nm) compared to the optical technique, the primary disadvantage of the piezoresistive detection method is the continuous thermal drift due to the heat generated by the current flow through the piezoresistor on the cantilever which might interfere with the long-term stability of MC response.

The other important electrical method is the self-sensing piezoelectric cantilevers in which a piezoelectric material (such as ZnO) is deposited on the MCs.[107–109] This detection mechanism takes advantage of the piezoelectric effect, where a change in mechanical stress (cantilever bending) causes the induction of transient charges finally translated into a change in voltage. Although this approach offers freedom from the bulky optical instrumentation and inconsistencies of laser alignment, it requires additional steps in the fabrication process to integrate a piezoelectric material into the MC thus making microfabrication process more expensive and cumbersome.

Another approach of cantilever deflection, capacitance method, is based on the principle that the change in the distance between the capacitor plates effectively changes the overall capacitance of the device. The deflection of the MC is measured by the changes in the capacitance between a conductor electrode and the MC substrate.[110,111] Despite its simplicity, this method suffers from undesired interference effects and the change in the dielectric medium between the capacitor plates which also changes the capacitance along with gradual discharge.

Very recently, Dravid and coworkers have introduced a novel method for the detection of the deflection of MCs where they have embedded a metal oxide semiconductor field effect transistor (MOSFET) in the base of the MC substrate.[112] The surface stress caused by the deflection of the MC results in an increase in the channel resistance due to the change in carrier mobility. Although the detection limit or maximum resolution (about 5 nm) currently achieved by the technique cannot even closely match that of the optical methods (< 0.1 nm), the technique offers the unique advantage of obtaining arrays of MCs with built-in detection elements enabling seamless monolithic integration.

3. Design and Fabrication of Bimaterial Structures

3.1. Fabrication of Microcantilevers

Traditionally, MC sensors have been fabricated by a photolithographic process and bulk micromachining or surface micromachining of single crystal silicon, polycrystalline silicon, silicon nitride, or silicon dioxide producing structures with a wide range of lengths from 100 to 500 μm (typically within 150–300 μm) and a thickness of 0.5 to 5 μm (typically, within 0.5–1 μm) (Fig. 7). These dimensions and materials result in spring constants ranging from 0.001 to 0.1 N m^{-1}.[113,114]

However, there have been several recent reports where other non-traditional materials such as metals, polymers, and nanocomposites have been employed to obtain cantilever structures instead of traditional microelectronic materials. For instance, lithographically defined polymer microcantilevers were fabricated from epoxy based photoresist (SU-8) with integrated gold layers serving as the piezoresistors.[115,116] The elastic modulus of SU-8 is nearly 40 times lower than silicon making the polymeric cantilevers significantly soft and support reversible deflections up to nearly 100 μm which is rarely sustainable with silicon cantilevers. However, it is important to note that the gauge factor of the SU-8 is nearly 50 times smaller than that of silicon, causing the effective piezoresistive sensitivity on the same order as silicon based cantilevers.

In an alternate method, polymer cantilevers with an aspect ratio close to 200 have been produced by injection molding of polymer melts such as polystyrene, polypropylene, and nanoclay/nylon composite into preformed commercially available micromolds.[117,118] In other study, Layer-by-Layer (LBL) technique, which offers nanometer control over the thickness of the polymer films, has proven to provide a multitude of soft free standing micromechanical structures with high degree of mechanical integrity and flexibility and very minute thickness unachievable by common microfabrication procedures.[17,73,119] LBL assembly of polycations, clay, and magnetite nanoparticles employed in this study produced 170 nm thick free standing composite cantilevers, which could be actuated by a magnetic field.[119]

3.2. Inorganic MC Coatings

As has been discussed above, for sensing applications the MC substrate must be coated with other materials (inorganic or organic) making them bimaterial structures. One of the earliest demonstration of gas sensors based on MCs was reported by Thundat et al.[120] In this study, MCs were coated with 20–50 nm gold to detect mercury vapor. The authors demonstrated that the adsorption of mercury vapor on the gold layer results in a change in the effective mass of the cantilever causing a detectable variation in the resonance frequency. Following this demonstration, there have been numerous reports where metals and metal oxides have applied on MCs as active absorbing layers or in contrast passivating layers causing preferential sorption of the analyte on one side of the cantilever.[110,115,121,122]

Metal coatings on MCs have been primarily fabricated by either sputter coating or thermal evaporation. Kadam et al have performed a comparative study of the Hg sensing ability of MCs with sputter coated and thermally evaporated Au films.[123] Although both the coatings resulted in bending in the same direction upon exposure to Hg, the deflection response of the thermally evaporated films tended to decay over time. Mertens et al. have studied the topological effects of thermally evaporated gold films on the molecular adsorption and nanomechanical response of the MCs.[124] They have found that smaller thicknesses and low deposition rates of Au result in large residual stress in the films due to the formation of well defined grain boundaries and this, in turn, leads to high sensitivity and reproducibility to molecular adsorption. For low deposition rates and thin films, the granular nanostructure of the Au films (shown in Fig. 8) provides enhanced surface area and confinement of analyte molecules in the nanocavities (interstices between the nanograins) to enhance the sensitivity of the MCs. In fact, two orders of magnitude increase in the sensitivity was observed by depositing Au on randomly grown silicon nanowires on the cantilever to enhance the surface area.[125]

3.3. Organic Layers as Responsive Coatings

While the initial demonstrations of the MC based sensor devices primarily relied on metal coatings due to the relatively straightforward coating processes, these bimaterial cantilevers are limited in their applications due to their limited chemical functionality and affinity to common targeted molecules. To enhance the functionality of the MC based sensors, numerous organic species have been applied as responsive coatings such as SAMs, biomolecules (DNA, specific antibodies, polypeptides, nucleotides), lipid layers, homopolymers, block copolymers, plasma polymers, polymer brushes, polymer/inorganic nanocomposites, hydrogels, and sol–gel layers to detect various physical, chemical and biological stimuli as will be discussed below. In particular, responsive organic coatings are important to optimize several key attributes, specifically high
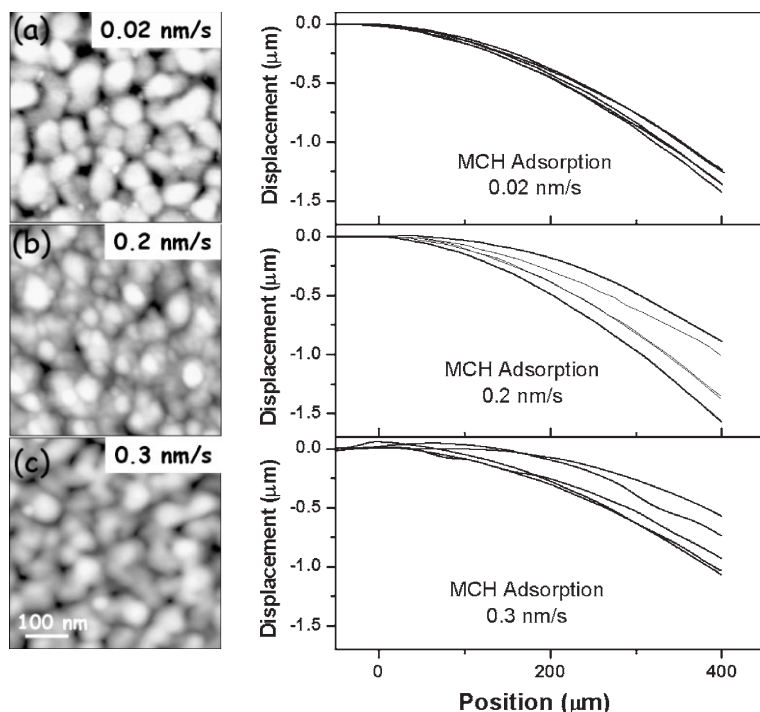
Figure 8. AFM topography images of thermal evaporated topmost gold layers and the corresponding static deflection of the MC for MCH adsorption at a rate of a) 0.02 nm s^{-1}, b) 0.2 nm s^{-1}, c) 0.3 nm s^{-1}. Reproduced with permission from [124]. Copyright 2007 American Institute of Physics.

sensitivity, selectivity, fast response time, wide dynamic range, and long shelf life critical for their ultimate performance as was discussed earlier. MCs are no exception to this and one has to consider several factors in designing the bimorph materials to preserve the inherent outstanding attributes of the transduction system.

3.3.1. Self-Assembled Monolayers

The application of SAMs to one side of MCs has been one of the prime techniques exploited to induce preferential adsorption of the analyte molecules. Surface modification with SAMs is inspired by the classical approach[22] in which the MC is initially coated with gold on one side by either sputtering or thermal evaporation. For example, MCs coated one-side with gold have been further modified with a thiol SAM to detect ppb level of cesium ions in the presence of high concentration of interfering potassium ions.[126] Following this initial demonstration, there have been several other impressive demonstrations where SAMs have been applied for the detection of metal ions, plastic explosives, nerve agents, and organic vapors.[127–132] SAMs offer a wide choice of chemical functionality for obtaining layers with specific affinity for the target analyte species, making the cantilever response highly selective. Robust and repeatable performance and selectivity, however, require a densely packed, high quality SAM on the cantilever surface. The cantilevers are immersed in dilute

solution (milli molar) of desired organic molecule (e.g., alkanethiols) in aqueous or organic solvent (e.g., water, ethanol) to enable the formation of the SAM on the metal surface. However, formation of densely packed SAMs on the surface of the cantilever by classical approach takes a long time often extending from tens of hours to a few days and is a subject of irregularities caused by external impurities.[127] Furthermore, the technique poses potential damage to the MCs due to significant stress caused by the surface tension especially during a drying stage.

As an alternate method, inkjet deposition of SAMs has been considered and implemented. In this method, microdroplets (5–25 μl) of solutions are delivered locally to the selected surface areas on the cantilever.[133,134] Evaporation of the droplets (within a few seconds) and subsequent removal of excess molecules by immersing the cantilever in solvent bath results in the fast formation of uniform SAMs on the surface of the MC. For example, Bietsch et al, have successfully demonstrated the alternate deposition of hydrophobic (octanedecanethiol) and hydrophilic (mercaptoundecanoic acid) monolayers on an array of eight MCs and subsequent differential condensation of water on the two sets of MCs making them essentially bi-functional array (Fig. 9).[133] The primary advantage of the inkjet printing over the classical self-assembly in solution is that the former is relatively fast and modestly destructive. Inkjet printing also provides a spatial resolution of a few hundred micrometers and thus additionally enables the functionalization of arrayed cantilevers with different functional layers, an important capability for multifunctional sensor fabrication.

3.3.2. Polymer Layers

Modification of MCs with thin polymer layers is probably the most common approach employed in applications involving chemical vapor sensing. Various methods such as drop casting,[135–138] spin coating,[139,140] inkjet printing,[133] spray coating,[141,142] capillary painting,[143] plasma polymerization,[144] *in situ* polymerization,[145–148] *grafting to* via SAM functionalization,[149] and matrix assisted pulsed laser evaporation (MAPLE)[150] have been adapted for modifying MCs.

While the response of the MCs coated from SAMs is due to the differential surface stress caused by changes in surface energy, the major contribution to the response of MCs coated with polymer layers is due to the solvation forces and swelling of the polymer layers. The sorption of the analyte molecules into the polymer film (swelling) results in relatively large differential stresses as compared with traditional SAM coatings. It is important to note that the magnitude of the response, the response time, and the selectivity of the MC sensors all scale with the thickness of the polymer layer. Various effects such
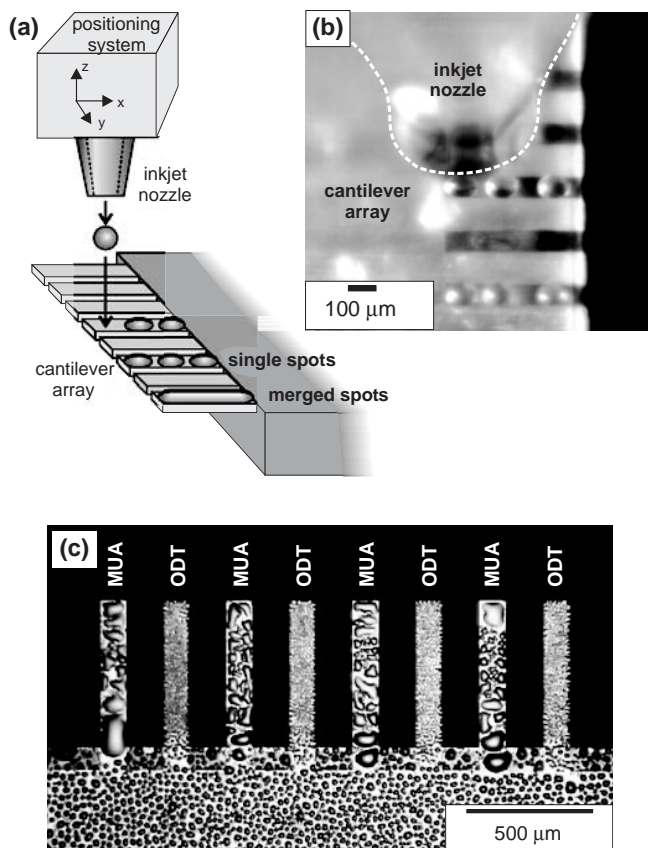
© 2008 WILEY-VCH Verlag GmbH & Co. KGaA, Weinheim

ADVANCED MATERIALS

Figure 9. Ink jet printing of responsive layers on an MC array (a); optical micrograph of the process (b); condensation of water on cantilever array coated with hydrophilic (MUA) and hydrophobic (ODT) layers (c). Reproduced with permission from [133]. Copyright 2004 IOP Publishing Ltd.

as electrostatic, osmotic, solvation, and steric contribute towards the response of the polymer layers to the variable chemical environment. For instance, Thundat et al have demonstrated a humidity sensor based on silicon nitride MCs modified with hygroscopic phosphoric acid and 23 nm gelatin layers.[151] In the case of the cantilevers coated with phosphoric acid, the MCs exhibited a decrease in the resonance frequency with increasing relative humidity due to the increase in the effective mass of the MC. On the other hand, the gelatin coated MCs exhibited an increase of the resonance frequency (explained as a change in k of the cantilever) correlated with a static deflection of the cantilever.

Drop casting, one of the most common methods for MC functionalization with polymer layers, involves micropipetting small droplets (few µl) of polymer solution on the cantilever and allowing solvent evaporation which leaves a thin polymer film on the cantilever. Although the technique is simple and easy to adapt, it provides almost no control over microstructure or thickness of the polymer film and hence results in poor reproducibility. Spray coating of the polymer solution also suffers from poor reproducibility and results in not very robust bimaterial MCs. Spin coating of the polymers usually results in uniform films with controlled thickness (optimized by the

spinning conditions and concentration of the polymer solution). However, spin coating the cantilever with polymer layers usually causes an unwanted deposition on the passive side of the MC substrate reducing differential stress not to mention the potential damage of the MC. A two step process, spin coating followed by focused ion beaming etching, has been commonly adapted to functionalize the MC on a single side. Although the technique results in a single side coating of the functional layer, it is time consuming and costly and not suited for functionalizing arrays of MCs with different polymers.

Plasma polymerization of organic precursors has recently been introduced for obtaining uniform polymer nanolayers acting as the active sensing component in thermal bimorphs. This technique is a solventless (dry) process, resulting in organic films with high solvent, scratch, and corrosion resistance combined with excellent thermal and chemical stability.[152,153] The underlying mechanism of plasma polymerization involves in organic species undergoing fragmentation in plasma, resulting in excited sub-monomer species, free radicals, and ions that can react with each other in the plasma zone, or at the nascent surface layer (Fig. 10). Depending upon parameters, these species can remain in a charged state inside the layer (charged polymer layer) or bond to each other to produce
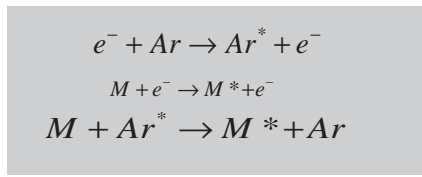
$$e^- + Ar \rightarrow Ar^* + e^-$$
$$M + e^- \rightarrow M* + e^-$$
$$M + Ar^* \rightarrow M* + Ar$$

Figure 10. Basic mechanisms of plasma polymerization and a typical reaction chamber for PECVD deposition.

highly crosslinked organic films.[154] Plasma polymerization offers the unique advantage of being able to polymerize numerous organic species, such as saturated alkanes, unsaturated alkenes, thiophenes, siloxanes, and fluorocarbon compounds. It is worth noting that in many cases, the resulting chemistry of these coatings is unique and often impossible to fabricate by traditional wet chemistry techniques.

Obviously, to retain the bimaterial-induced bending effect, the plasma polymerization must be controlled so that only one side of the MC is modified. This can be done in single step, in-vacuum process, as opposed to the conventional wet-fabricated coatings discussed earlier. One of the other advantages of the plasma polymerization technique is the excellent adhesion of the coatings to numerous substrates, which is highly desirable for stress transfer to the MC.

Figure 11 shows the AFM image of a spin coated polymethacrylonitrile (PMAN) film in comparison with plasma polymerized methacrylonitrile (ppMAN) film of the same nominal chemical composition.[144] While the spin coated film exhibits smooth and featureless surface morphology the
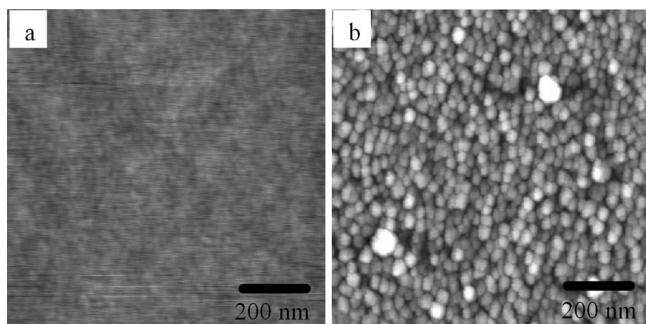
Figure 11. AFM topography images of: (a) spin coated and (b) plasma polymerized PMAN showing the smooth and featureless morphology of spin coated films as opposed to the granular domains of the plasma polymerized films [156].

ppMAN film shows a characteristic granular morphology with highly developed nanoporous structure. This is similar to the metal films deposited at small rates as previously discussed in which well defined grain boundaries in the case of the metals deposited at smaller rates offer the advantage of the enhanced surface area and locked in residual stress. The physical properties of the plasma polymerized organic films, such as the degree of crosslinking, the elastic modulus, internal (residual) stress, thermal expansion, adhesion, and surface morphology can be controlled by adjusting deposition parameters.[156] This control includes rate of deposition of the monomer, power of plasma source, pressure in the chamber, and flow gas type and rate, as have been comprehensively reviewed by Yasuda.[157]

Selection of the responsive polymer coating which is highly sensitive and selective (at least partially) is the most important design criterion of polymer based MC sensors. It is important to note that selectivity, response time, and reversibility are dictated by the thermodynamics and kinetics of the responsive material interacting with the analyte molecules, which frequently leads to a compromise between high selectivity, typically associated with strong interactions, and complete reversibility requiring weak interactions. Although no systematic studies on this subject exist in the context of MC based sensors with various polymeric coatings, significant efforts in understanding the correlation between the analyte origin and the polymer coating has been done for popular piezoelectric devices such as surface acoustic wave (SAW) microsensors and thickness shear mode (TSM) resonators.[158,159]

For instance, the partition coefficient which is defined as the ratio of the concentration of the solute (analyte molecules) in the sensitive coating to the concentration of the analyte in the vapor phase is the single most important parameter in the selection of the sensitive layer in these sensors. Indeed, experimental results prove that the shift in the resonance frequency of the SAW devices is directly proportional to the partition coefficient.[160] Linear solvation energy relationship (LSER) has been applied to compute the partition coefficients of the analyte/coating layer by taking hydrogen bonding, dipolarity, polarizability and dispersion effects into account thus providing a rich database for selection.[161,162] The

readers are referred to an excellent review on the subject for further insight.[163]

It is reasonable to suggest that the design principles established in these gravimetric devices can form good initial guidelines for designing MC based sensors; however, care should be taken while adapting these material selection schemes without modification. For example, it is known that elastomeric materials are advantageous compared to glassy materials in SAW devices due to the better reversibility and faster response time. It is also known, however, that the higher the elastic modulus of the coating layer the greater the differential stresses and thus higher static deflection in MC based sensors making elastomeric materials not very suitable for bimaterial designs with high sensitivity. Thus, for bimaterial MCs, structure design rules need to be optimized in accordance to the specific requirements.

It is also important to remember that the magnitude of the response, the response time, and the selectivity of the MC sensors inevitably scale with the thickness of the coatings. In recent study, Betts et al. have addressed the issue of the sensitivity and selectivity of MCs coated with poly(cyanopropylsiloxane) (SP-2340) of different thickness.[139] The authors have observed a general trend of decreasing signal to noise ratio (SNR) for various organic vapors with increasing film thickness. The selectivity factor defined as the ratio of the response to analyte vapor to a standard interfering vapor (pentane in this case) exhibited a modest increase (50 %) as well when thickness was increased from 50 nm to 100 nm followed by a slight decrease for thicker coatings. Even more recently, Lochon et al have shown that the sensitivity (measured in terms of a frequency shift) of poly(etherurethane) coated MCs increases linearly with thickness of the coatings (1–20 μm).[142] However, the thermal noise of the MCs also increased significantly for MCs with the thicker coating making the detection limit to stay constant or even worsening with the increase in the coating thickness. Moreover, they have also shown that the increase in the coating thickness causes an increase in the response time, a highly undesirable output. In other study, Zhao et al have reported the coating thickness dependence of PS coated MC bimaterial structures.[143] They have shown that the interfacial tension, which remains constant for coatings with different thicknesses dominates the thermal response of the bimaterial MCs for thinner coatings (< 20 nm) while for higher thickness the thermal expansion coefficient dictates the resulting static deflection.

4. Performance of Bimaterial Structure for Various Applications

4.1. Uncooled Thermal Sensors

The detection of infrared (IR) radiation in particular, the wavelength regions from 3 to 5 μm and 8 to 14 μm, is of importance since atmospheric absorption in these regions is especially low.[164,165] According to the transduction princi-

ples, IR detectors can be classified broadly as quantum (opto-electronic) and thermal.[166–168] Thermal IR detectors, in turn, can be based on pyroelectric,[169] thermoelectric, thermoresistive (bolometers),[170–174] and micromechanical transducers.[104,175–183] Bimaterial microcantilevers can also be used to turn heat into a mechanical response and can be referred to as thermo-mechanical detectors. An important advantage of thermo-mechanical detectors is that they are essentially free of intrinsic electronic noise and can be combined with a number of different readout techniques with extremely high sensitivity.

The bimaterial design can be exploited for IR detection by fabricating microcantilevers whereby bending of a cantilever upon incident radiation results from a mismatch in thermal expansion coefficients (a) of the materials as was discussed above.[184,185] This approach was pioneered by Barnes and Gimzewski when they coated MCs with a metal (as the sensing active layer) to form the bimorph.[186] Later, Datskos et al. made the point that 2D arrays of these heat sensitive cantilevers can serve as thermal imaging devices.[104,175] The ideal bimaterial properties of a MC engineered for IR sensing include large mismatch of a and thermal conductivity (λ) between the two materials with one of the materials having extremely low λ. Low residual stresses are useful to reduce non-thermal bending and one of the materials should absorb in the desired IR range. However, Tsukruk and co workers have demonstrated that trapped residual stress in the coating layers can significantly enhance the response of the bimaterial structures as will be discussed later.[144]

In one of the recent designs, Quate et al. used silicon cantilevers exotically shaped in a flat spiral with an aluminum coating to complete the bimorph.[187] Datskos et al. developed a microcantilever bimorph with silicon as a substrate, and a 150 nm gold coating as the high a component that exhibited temperature sensitivity of 0.4 °C.[188] Majumdar et al. applied bimaterial cantilevers of silicon nitride and gold into a complicated comb-like MEMS structure, which resulted in sensitivity of 3–5 °K.[189] Sarcon Microsystems in cooperation with Oak Ridge National Laboratory (ORNL) have developed bimaterial cantilevers with a theoretical sensitivity approaching 5 mK, which is the lowest value reported for uncooled IR detectors based on metal-coated cantilevers (Fig. 12).[190] In their design, SiC was the low (a) component, again being combined with aluminum as the high (a) layer. In Figure 12 we show an example of an IR imaging system based on an array of 256×256 bimaterial MCs.[155] An optical readout was used to simultaneously interrogate all the MCs. Figure 12c shows an example of a thermal image of a human obtained using this MC array with an optical readout.

Considering that the difference in thermal expansion coefficients for metal-ceramic bimaterial designs discussed so far is inherently limited ($\Delta a < 20 \times 10^{-6}$ K^{-1}), the polymer-ceramic bimaterial cantilevers have been suggested to dramatically enhance thermally induced bending due to much more efficient actuation of readily expandable polymer nanolayers with $\Delta a = 200 \times 10^{-6}$ K^{-1}, combined with low thermal conductivity.[149] Thus, polymer-nanoparticle composite structures have been introduced with a combination of polymer brush layer, silver nanoparticles, and carbon nanotubes to enhance IR
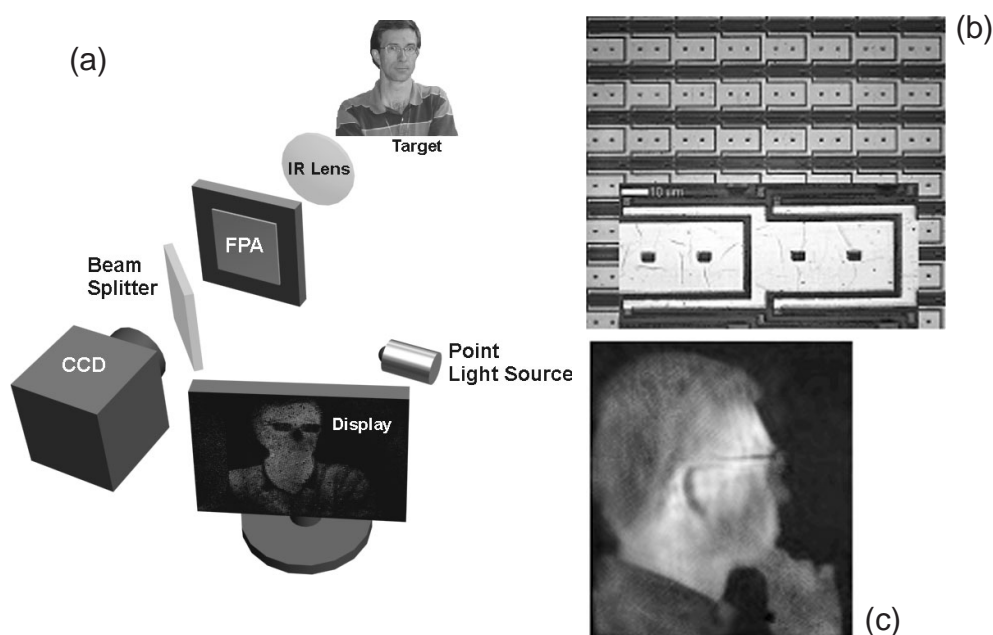

Figure 12. a) Schematic illustration of the components and the arrangement of the optical readout of a 256 × 256 array of bimaterial MCs. b) Part of a fabricated 256 × 256 array. The selected geometry is characterized by a high fill factor and relaxed design rules. c) Example of a thermal image of a human obtained using an optical readout. Reproduced from [155] with permission. Copyright 2006, American Institute of Physics.

ADVANCED MATERIALS

adsorption and reinforce the nanocomposite coating (Fig. 13). The application of such a reinforced nanocomposite coating with high (*a*) allowed to achieve nearly fourfold improvement (theoretical, noise-limited detection limit of 0.5 mK) in the
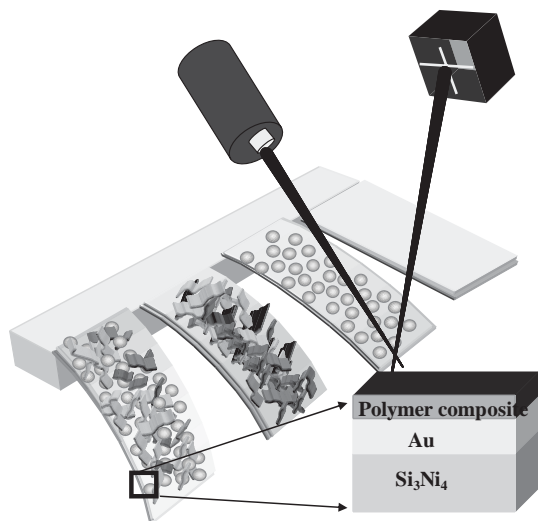

Figure 13. Schematic of trilayered MCs coated with polymer nanocomposite for IR sensing application [149].

thermal sensitivity compared to the metal coated counterparts.[149] Although there was substantial improvement in the sensitivity of the thermal bimorphs, the wet grafting technique employed to modify the MCs was tedious, frequently resulting in cantilever damage, and was not compatible with traditional microfabrication technology.

To overcome these shortcomings, plasma polymers have been employed as actuators in MC thermal bimorphs.[144] Plasma polymerized styrene (ppS) coated MCs exhibited a deflection of nearly 2 nm mK^{-1} making the theoretical detection limit to be 0.2 mK (Fig. 14a–c). It is interesting to note that the response of the plasma polymer coated MCs was in opposite to the thermal expansion since the variation of the internal stress in the polymer layer with temperature dominates the bending. In fact, the estimation of the internal stress in plasma polymerized coatings gives differential stresses close to 100 MPa, which is a very high value indicating high compression of the polymer layer at room temperature. It is suggested that the high crosslink density of the polymer layer and their chemical grafting at the interface should provide enhanced mechanical and thermal stability of these layers even under such high stress. Calculation of the differential surface stresses with finite element analysis (FEA, Fig. 14d) gives a value of 10 N m^{-1}, which is much higher than stresses usually generated by grafting polymer layers (usually within 0.3–1 N m^{-1}) and resulting from molecular adsorption (< 0.2 N m^{-1}).[191] Moreover, it shows that compressive stress within the polymer layer reaches 60 MPa, and is balanced by the tensile stress exactly at the polymer-silicon interface combined with compressive stress at a bare silicon surface.
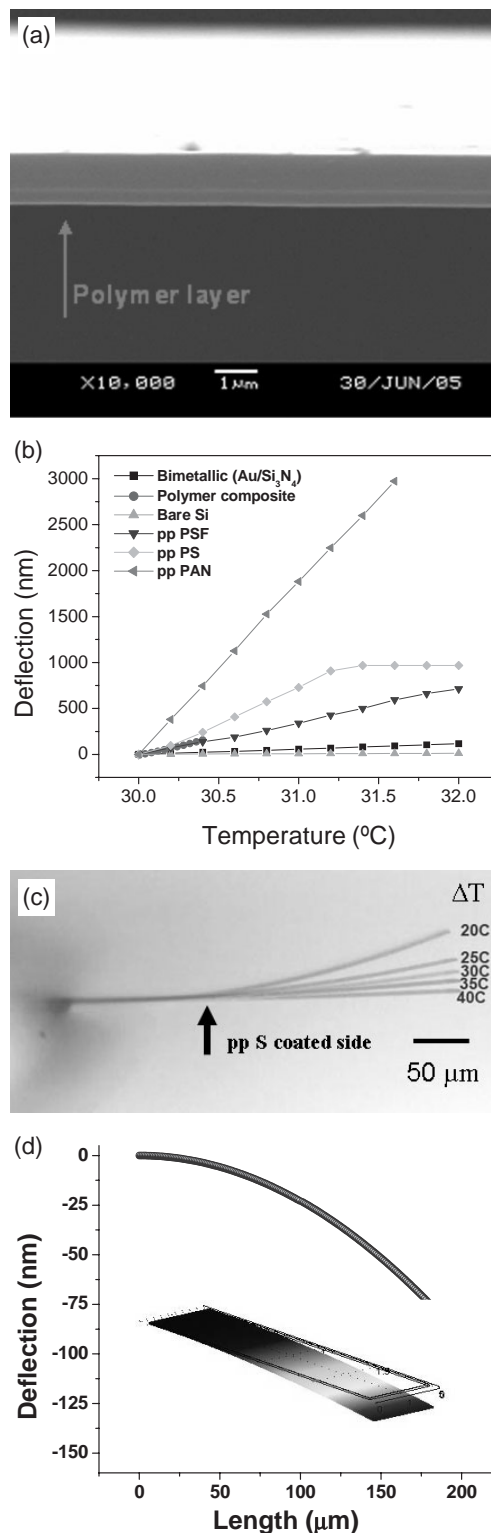

Figure 14. a) SEM image of MC coated on a single side with ppS. b) Deflection response to temperature for MCs (350 μm ×35 μm × 1 μm) coated with gold, polymer composite (Polyacrylonitrile/carbon nanotube), Plasma polymerized pentafluorostyrene, styrene, acrylonitrile, and uncoated reference [144,149]. c) Overlapped optical micrographs of the ppS-MC at various temperatures [144]. d) FEA analysis showing the deflection profile of the MC for 1K change in temperature [149].

4.2. Probing Kinetics of Dynamic Systems

Commonly used instruments for observing the kinetics of biomolecular interactions on a surface include surface plasmon resonance[192] and quartz crystal microbalance with dissipation monitoring (QCM-D).[193] Due to the extreme sensitivity of MC transduction (nearly 3 orders higher mass sensitivity than QCM[194]), it has attracted considerable attention for probing the dynamics of physical and chemical processes occurring at molecular levels. The first report of monitoring a chemical reaction on the surface of a MC was done by Gimzewski et al., in which they have monitored the catalytic conversion of $H_2 + O_2$ to H_2O on platinum coated MCs introducing the concept of MC based microcalorimeter. The kinetics of chemisorption of alkanethiols on gold coated MCs has been investigated by various groups.[191,195,196] Berger et al have observed a linear increase in the surface stress at the monolayer with the length of the alkyl chain of the molecules (see Fig. 15). It is important to note that the deflection of MCs during the assembly process was dominated by the differential surface stress while the thermal and gravimetric effects were negligible.[195]

MC-based sensing has also been employed to probe swelling of polymer layers[197–199], self assembly of polyelectrolyte monolayers,[194] formation of lipid layers,[200] and conformational changes of proteins.[201,202] It is worth noting that since
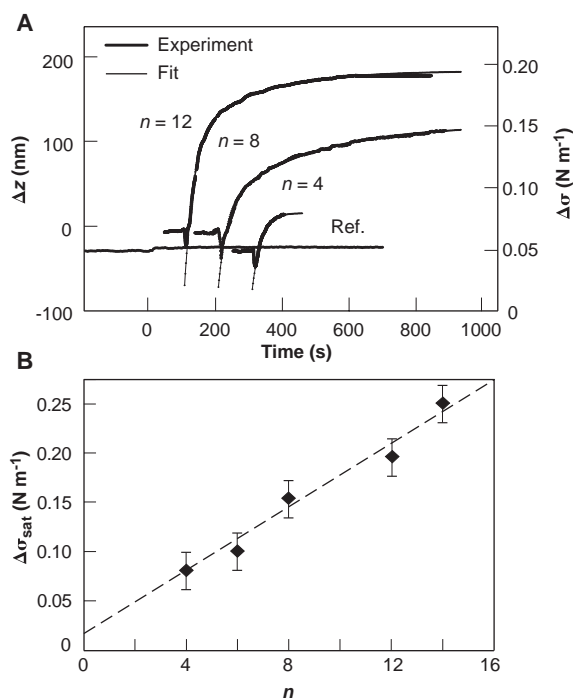

Figure 15. a) Deflection (Δz) and Surface stress (Δs) of MC sensors plotted as a function of time for the chemisorption of alkanethiols of various alkyl chain lengths; b) Plot depicting the surface stress at saturation coverage vs. alkyl chain length (n). Reproduced with permission from [195]. Copyright 1997 American Association for the Advancement of Science.

MCs are sensitive to the slightest environmental fluctuations due to flow and thermal gradients, data acquisition during analyte introduction in liquids often precludes observation of the associated kinetics within a given time interval. The time necessary for full equilibration ranges between minutes and hours for deflection sensing.[200,203–205] A time delay also exists between molecular binding and generation of sufficient surface stress to initiate measurable cantilever deflections which also complicates the experimental results.

4.3. Selective Binding Events

Over the past ten years, microcantilevers have also been applied as biosensors as stand-alone structures and in arrays for detecting protein interactions,[203,206–213] DNA binding,[116,214–216] and microorganism behavior on surfaces.[217–219] By specifically functionalizing only one microcantilever surface, either the frequency or deflection mode can be used to detect specific biomolecular binding events. The selectivity of the microcantilever response is based on the specificity of the capture molecule. In the following, two representative examples will be highlighted. Both approaches used a standard AFM setup to measure deflection resulting from oxidation of glucose and binding of prostate-specific antigen (PSA).

In the case of a glucose sensor, glucose oxidase (GO_x) was immobilized on a single gold coated rectangular microcantilever.[192] The study showed the ability of MCs to detect physiologically relevant levels of glucose, but not yet conduct selective detection from a mixture of proteins and plasma normally present in a blood sample. Selectivity is decreased in this electrochemical setup due to the presence of interfering electroactive species (e.g., ascorbic acid, catechol, or uric acid). Microcantilever technology, however, does not detect any such spectator species, and thus provides improved selectivity. Although these results are promising, there are still reproducibility concerns, as the microcantilever response declined steadily with each subsequent exposure to glucose due to hydrogen peroxide production during the enzymatic reaction, which can corrode the enzyme layer.

In another study, Wu et al. used microcantilevers to detect PSA from a mixture of blood proteins.[203] Commercially available V-shaped, gold-coated MCs were decorated with a layer of anti-PSA antibody. Significant deflection was observed upon binding of free PSA. When exposed to concentrations spanning the diagnostically relevant range (0.2 ng ml^{-1}–60 µg ml^{-1}), the microcantilevers showed a distinct deflection in a background of 1 mg ml^{-1} BSA (Fig. 16). Deflection at 60 ng ml^{-1} versus 6 ng ml^{-1} was also clearly distinguishable even in the presence of 1 mg ml^{-1} human serum albumin. Changes in MC geometry resulted in shifted deflections for the same concentration of PSA. The authors found that surface stress, however, was geometry-independent and directly related to PSA concentration as shown in Figure 16. Nonspecific interactions had very little effect on deflection, suggesting that surface stress is a sensitive reporter of specific PSA binding.
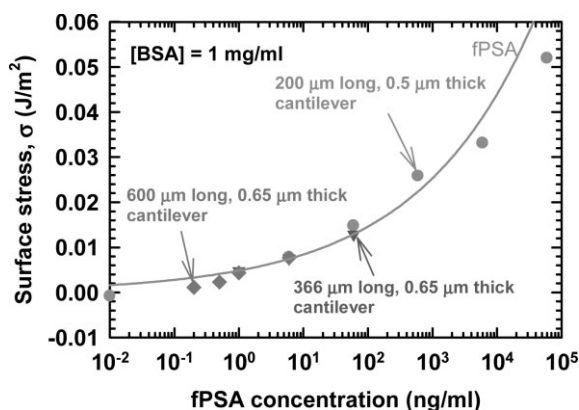
Figure 16. Surface stress is directly related to free PSA concentration, regardless of microcantilever geometry. Reproduced with permission from [203]. Copyright 2001 Nature Publishing Group.

The high selectivity of these assays resides in the specificity of the biomolecular reactions occurring on the properly modified microcantilever surface. Unlike electrochemical or labeling detection methods, the free energy change resulting from molecular recognition binding is directly translated into a mechanical deflection, reducing the effects of sources of interference (e.g., optical, electrochemical). Smaller cantilevers, increasing ligand surface density, and decreasing surface roughness promise to increase detection sensitivity. The use of differential signal by employing reference, unmodified cantilevers may further increase sensitivity, resolution and decrease errors from nonspecific interactions.

4.4. Liquid Composition

Microcantilevers modified with stimulus-responsive polymers provide an attractive approach to characterize changes in the liquid composition surrounding the cantilever. To this end, pH, salt, and solvent sensitive polymers and biomacromolecules have been grafted to cantilever surfaces and detection has been conducted directly in a liquid phase.[147,148,204]

For example, Abu-Lail et al. synthesized pNIPAAM brushes on the gold coated surface of a commercially available V-shaped cantilever, leaving the bottom side uncoated.[147] Due to solvent-induced conformational changes in the brush layer, the cantilever deflection was large and reversible. Surprisingly, the change in surface stress between brushes in good (H_2O) and poor (H_2O and MeOH) solvents were approximately independent of brush height. This suggests that ultrathin brushes (81 nm when swollen) are sufficient to report changes in solvent conditions. Changes in the solvent pH were measured by pH-sensitive pNIPAAM–vinylimidazole copolymer brush, grafted to the cantilever surface by surface initiated polymerization. Although conformational changes in the copolymer brush layer translate into large cantilever deflections, the equilibration time (on the order of 1 hour) and the sensitivity to temperature fluctuations were cited as draw-

backs of monitoring deflection in liquid. Associated with the conformational change in the polymer brush is also a significant change in the amount of viscously coupled water. The concomitant apparent mass changes when the polymer brush undergoes a phase transition, which could be detected by tracking the shift in the resonance frequency. Although this approach is fast, as it does not rely on precise static deflection measurements, viscous damping effects from operation in liquid impede sensitivity and compromise data interpretation.

Similar results were observed when elastin-like-polypeptides (ELPs) were grafted to the top surface of a gold-coated V-shaped cantilever. Valiaev et al. detected ELP swelling and collapse triggered by changes in the ionic strength and pH as displayed in Figure 17.[204] Resulting changes in surface stress, however, were smaller than those for pNIPAAM, most likely due to the decreasing surface density from the grafting-to pro-
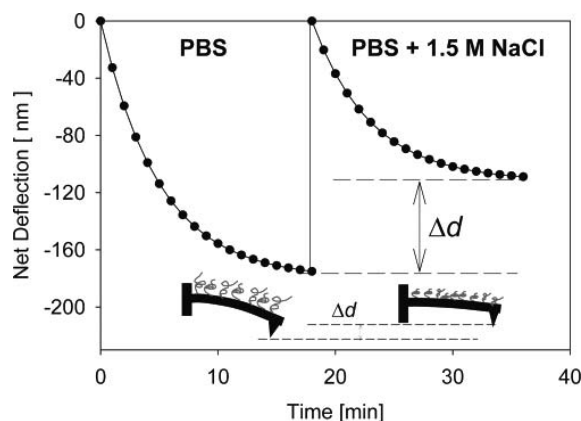

Figure 17. Net microcantilever deflection plotted as a function of time for two different ionic strengths (PBS and PBS + 1.5 M NaCl). Net deflection is determined as the difference between the deflection of a microcantilever with end-grafted ELP and deflection of a bare gold reference microcantilever under the same solution conditions. Δd indicates the effective difference in cantilever deflection at steady state. Reproduced with permission from [204]. Copyright 2007 American Chemical Society.

cedure. While lower grafting density decreases sensitivity, ELPs offer many advantages over synthetic polymers. They are genetically engineered with known amino acid sequence and precise molecular weight. The phase transition behavior is also tunable by varying the amino acid sequence and the molecular weight of the polypeptides.

4.5. Biological Macromolecules

Microcantilevers have been used to study not only binding of specific ligands onto functionalized surfaces, but also to monitor conformation of biological macromolecules after adsorption on the surface. Since microcantilever detection does not rely on a particular material substrate, a wide variety of different surface functionalities can be presented. Thus a range of interactions can be screened and monitored relative-

ly easily. In fact, protein interactions [203,206–213], DNA hybridization,[214–216] protein conformations,[201,220] and more recently lipid bilayer formation,[200] have all been observed using microcantilever sensors.

DNA hybridization was one of the first processes studied using functionalized microcantilevers in liquid. Fritz et al.[214] showed that a single base pair mismatch could be detected by observing microcantilever nanoscale deflection. In these experiments, a linear array of eight rectangular microcantilevers, each functionalized with a different oligonucleotide base sequence was employed (Fig. 18). By determining the differential deflections between adjacent cantilevers, confounding effects such as nonspecific interactions were significantly
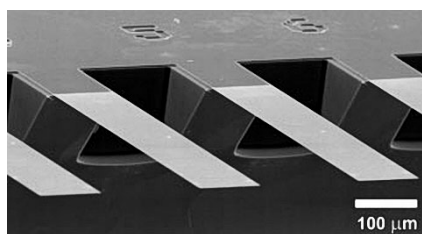

Figure 18. SEM micrograph of a section of a microfabricated silicon cantilever array (eight cantilevers, each 1 μm thick, 500 μm long, and 100 μm wide, with a pitch of 250 μm). Reproduced with permission from [214]. Copyright 2000 American Association for the Advancement of Science.

minimized and thus the sensitivity to a single pairing event has been optimized. Moreover, it was observed that the cantilevers were reusable after cleaving the bound DNA with urea.

Many subsequent studies have expanded this initial work beyond the initial scope. For example, Braun et al.[220] used microcantilevers to monitor the conformational changes in membrane-bound bacteriorhodpsin (bR) on a gold surface. Ink jet spotting was used to deposit bR on a linear array of eight gold coated rectangular microcantilevers, where some cantilevers were also left pristine to serve as a reference. Cantilever deflection was then monitored using a standard optical photodiode system. bR was pre-bleached by removing various degrees of retinal, an internally bound ligand, resulting in different bR conformations. Hydrolysis of retinal was also simulated *in situ* by the addition of hydroxylamine. It was found that 33 % pre-bleached bR resulted in a much lower deflection upon addition of hydroxylamine when compared to unbleached bR. As noted in other studies and mentioned briefly above, the cantilever deflection was unstable during flow compromising stability, and data were thus recorded before and after bleaching. Since nonspecific adsorption of hydroxylamine was observed on both bR and control cantilevers, the differential deflection was thought to be independent of nonspecific binding, and was caused by conformational changes due to retinal removal. This conformational change in bR was postulated to result in the expansion of the membrane patches, further altering the surface stress and tuning cantilever deflection.

Furthermore, vesicle fusion and lipid bilayer formation have been observed using microcantilever deflection in liquid. In these experiments, the deflection of an MC linear array was monitored by individual laser beams. To observe physisorbed bilayer formation on the bottom SiO_2 surface, the top gold surface was coated with 2-mercaptoethanol to minimize vesicle fusion there. After incubating with vesicles and flushing with buffer, tensile stresses developed due to the bilayer formation led to the cantilever deflection on the order of 80 nm, corresponding to a low but detectable surface stress of 30 mN m^{-1}. In another experiment, chemisorbed bilayer formation was observed on the top gold surface with thiolated lipids.[200] This bilayer formation resulted in the compressive stress causing the cantilever deflection in the hundreds of nanometers indicating ten times the surface stresses from simply physisorbed bilayers. When mixed with unmodified lipids, the deflection response decreased proportionally. The "pinning" of the bilayer was postulated to increase the surface stress, and the overall increase was similar to that seen for alkylthiol SAMs.

4.6. Cells, Microorganisms

Microcantilevers have also been employed to characterize the behavior of microorganisms on solid substrates, a very intriguing mode of observation. Virus mass,[218] *E. Coli* activity[217] and fungal growth have all been recorded by monitoring shifts in the resonance frequency. Both Gfeller et al. and Nugaeva et al. performed these studies at high relative humidity (RH > 93 %), but not in truly liquid environment. Limitations in surface grafting density, and the option to observe microorganism behavior in gaseous environments favored the faster detection mode of resonance frequency monitoring. Both studies relied again on a linear array of eight microcantilevers with individual cantilevers functionalized using quartz microcapillaries. Gfeller et al.[217] also used MCs coated with agarose to monitor *E. Coli* growth behavior. The major growth phases of *E. Coli* present in solution were again observed through easily detectable resonance frequency shifts over the period of several hours (Fig. 19). During the different development phases, growth and spreading of the bacteria, the change in the resonance frequency was due to the uptake of water from the nutritive medium into the agarose layer to compensate for proteins, salts, and carbohydrates taken up by the growing bacteria with the overall mass transfer monitored with cantilever deflection. Bacterial growth has been also monitored with the addition of 10 μg ml^{-1} kanamycin, an antibiotic which inhibits *E. coli* growth. Although frequency shifts were fairly large (over 600 Hz over an eight hour time period, Fig. 19), no change in the quality factor was observed, suggesting that no change in viscous damping occurred. The authors suggested that cantilevers with higher resonance frequencies would further increase the sensitivity to observe fine details of the bacterial growth.
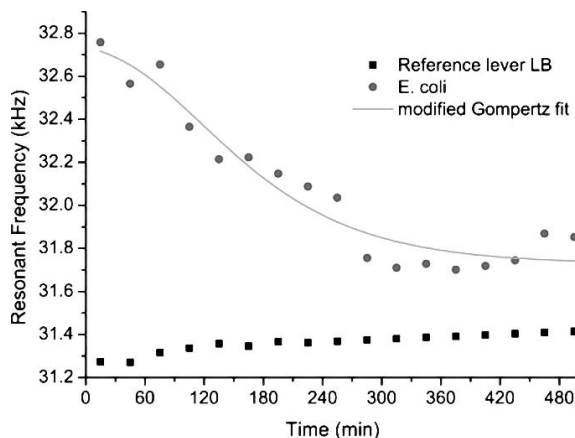
ADVANCED MATERIALS

Figure 19. For microcantilevers coated with *E. coli*, the lag, exponential growth, and stationary phases were evident in deflection measurements compared to a reference lever in medium. Reproduced with permission from [217]. Copyright 2005 American Society for Microbiology.

4.7. Chemical Vapor Detection

Sensors for a reliable detection of solvent vapors are important in chemical process technology, e.g., for safe handling during storage and transport of large amounts of solvents in a container. A fast test is required to verify that actually the solvent is in the container. Indeed, the MC bending specific to the interaction between solvent vapor and polymer with respect to time- and magnitude evolution was exploited for vapor monitoring.[137,141,146,221–236] In a typical laboratory test, 0.1 ml of various solvents was placed in vials, and the vapor from the headspace above the liquid was sampled using microcantilever sensor arrays, operated in static deflection mode as a kind of artificial nose (Fig. 20a).[141] Detection of vapors takes place via diffusion of the analyte molecules into the polymer coating, resulting in a swelling of the polymer and bending of the cantilever. Each cantilever is coated with a different polymer or polymer blend to provide for high selectivity (see Fig. 20). Examples of cantilever deflection traces upon injection of dichloromethane vapor at 50 s for 10 s are shown in Figure 20b (Data courtesy by Marko Baller, ORNL). The cantilever deflections at the time points t1 to t5 describe the time-development of the curves in a reduced data set, i.e., 8 x 5 = 40 cantilever deflection amplitudes ('fingerprint') that account for a measurement data set (Fig. 20). This data set is then evaluated using PCA techniques, extracting the most dominant deviations in the responses for the various vapors (Fig. 20c).[141] The axes refer to the projections of the multidimensional datasets into two dimensions (principal components). Vapor injections involved water, ethanol, dichloromethane and toluene. The PCA plot shows well separated clusters of measurements indicating clear identification of vapor samples.

In another example, MCs coated with 300 nm of plasma polymerized methacrylonitrile (ppMAN) exhibited nearly
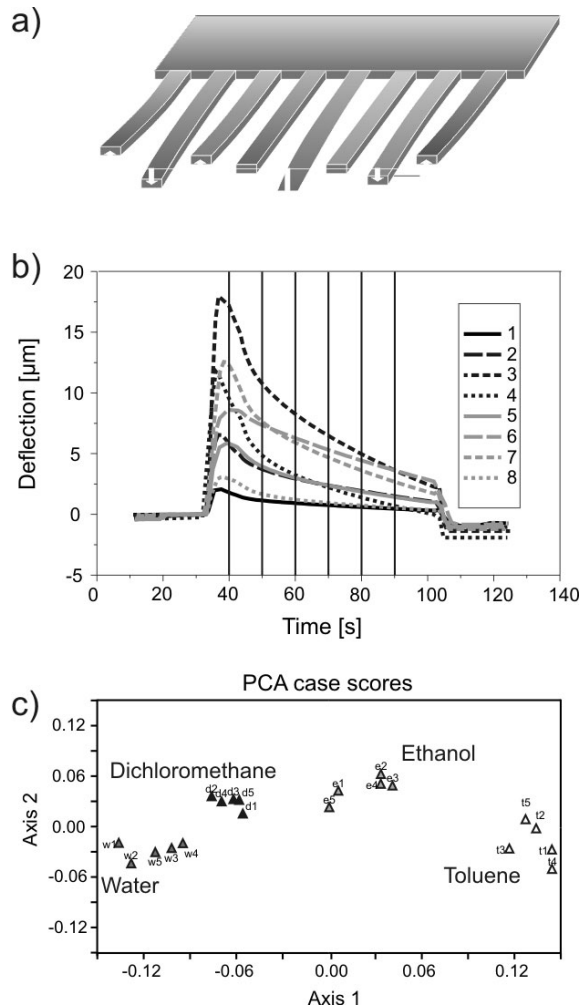

Figure 20. a) Schematic of a cantilever array functionalized with polymers exhibiting a deflection pattern which can be exploited for artificial nose application b) Cantilever deflection traces during exposure of a polymer-coated cantilever array to dichloromethane vapor. The following polymers were used: 1 = PVP, 2 = PVP/PU/PS/PMMA, 3 = PU/PS/PMMA, 4 = PU/PS, 5 = PU, 6 = PS/ PMMA, 7 = PS, 8 = PMMA. PVP = polyvinylpyridine, PU = polyurethane, PS = polystyrene, PMMA = polymethyl methacrylate. (c) PCA plot demonstrating the recognition capability of the cantilever-array [141].

3.5 μm static deflection for 1 % change in relative humidity making the detection limit at a very low value of 10 ppb or differences in 0.00005 % in relative humidity (Fig. 21a and b).[237] These MCs exhibited a monotonous deflection response from 5 % to 70 % (total deflection > 200 μm) with very small hysteresis (< 2 %). The MCs also exhibited an extremely stable response to water vapor over long storage time (nearly 2 years) with less than 5 % variation. The MCs coated with different plasma polymers have been exploited for organic vapor and plastic explosive detection and proved to be highly sensitive, very robust, and extremely selective with the response spanning four orders of magnitude to various analyte molecules (Fig. 21d). Moreover, under certain conditions,
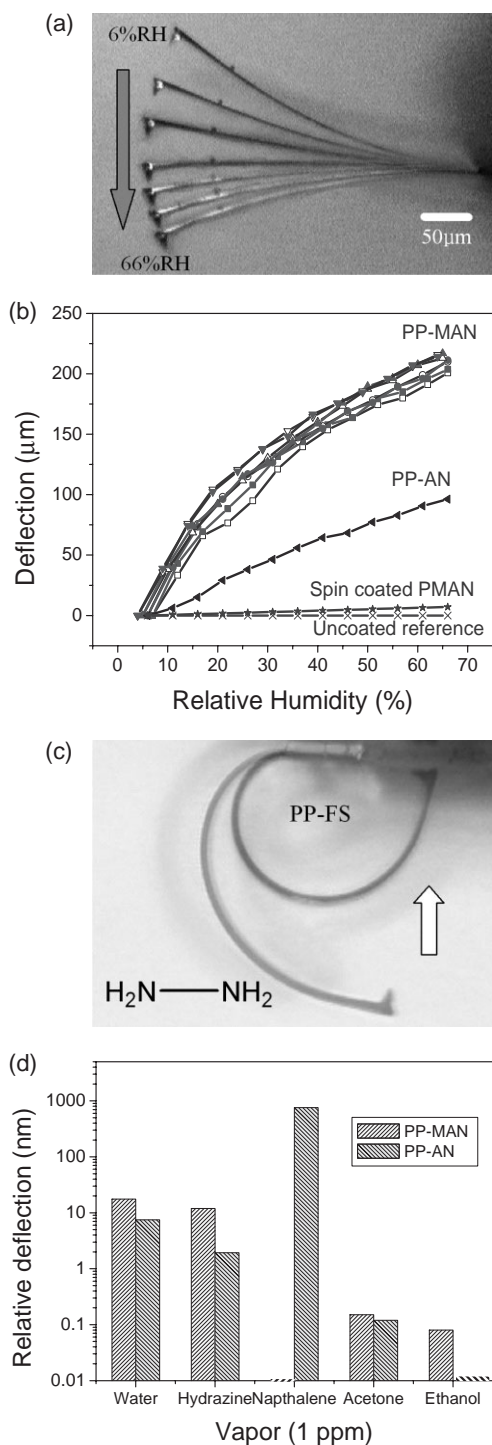
ADVANCED MATERIALS

Figure 21. a) Optical images showing the bending of the ppMAN-coated cantilever for humidity changing from 6 % to 66 % RH at an interval of 10 % RH with deflection at 6 % taken a reference point. b) The deflection vs. humidity of cantilevers coated with ppMAN, ppAN, spin-coated PMAN and a bare silicon cantilever. Empty symbols indicate humidification and corresponding filled symbols indicate desiccation: triangles (5th consecutive cycle), inverted triangles (10th consecutive cycle), squares (four months after fabrication), circles (after 18 months). c) Optical image of a ppSF-coated MC bent nearly 180° due to high residual stress and response to hydrazine vapor. d) Deflection response of ppAN and ppMAN to 1ppm concentration of different vapors [237].

the interaction of plasma polymer coated cantilever with analytes resulted in such strong stress that the MC becomes completely bent (Fig. 21c).

It is suggested that, unlike conventional bimaterial structures, which rely on small differences in the surface tension for active and passive sides, plasma polymerized coating facilitates a mechanism involving large interfacial stresses causing inherently higher bending forces. High stress at the plasma polymer-silicon interface (reaching tens of MPa or 5–10 N m^{-1}) facilitates large micrometer-scale responses to external stimuli, such as polymer swelling. The exceptional performance of the plasma polymerized ppMAN nanocoating is likely caused by the peculiar nanodomain morphology, the nanoporous structure, and the presence of polar segments and hydrophobic methyl groups in a highly randomized crosslinked chemical topology, all of which facilitate fast uptake and removal of water molecules. The reported sensitivity of 3500 nm/1 % RH for plasma polymerized cantilevers is more than two orders of magnitude better than that achieved before, indicating efficient transfer of swelling-induced stress to the polymer-inorganic interface. The most interesting aspect of this type of MCs is the very fast response time of the plasma polymers which is essentially instantaneous (<80 ms) for even large humidity changes (Fig. 22).

4.8. Explosives Trace Detection

Although explosive detection falls into the broad category of chemical sensing, it is unique due not only to the exigency in combating the potential threats but also to the extremely high sensitivity requirements. Threats can be of chemical, biological, radioactive or explosive in nature. Preventive countermeasures require inexpensive, highly selective and very sensitive small sensors that can be mass-produced and microfabricated. Such low cost sensors could be arranged as a sensor grid for large area coverage of sensitive infrastructure, like airports, public buildings, or traffic infrastructure. Microfabricated detectors for explosives will be very useful as compact versions of established monitoring technologies like the ion mobility spectrometer[238] or nuclear quadrupole resonance[239] have been developed, but are not likely to be miniaturized further.

Two approaches have been adapted for the detection of explosives using MCs: 1) static or dynamic mode of operation where MCs are functionalized with SAMs or polymer layers to achieve selective binding.[128,150,237,240] 2) Microdeflagration of the explosives on the MC surface.[241–243] Several approaches to detect dangerous chemicals are described in literature: photomechanical chemical microsensors based on adsorption-induced and photo-induced stress changes due to the presence of diisopropyl methyl phosphonate (DIMP), which is a model compound for phosphorous-containing chemical warfare agents, and trinitrotoluene (TNT).[223] Further explosives frequently used include pentaerythritol tetranitrate (PETN) and hexahydro-1,3,5-triazine (RDX).[128] These compounds are
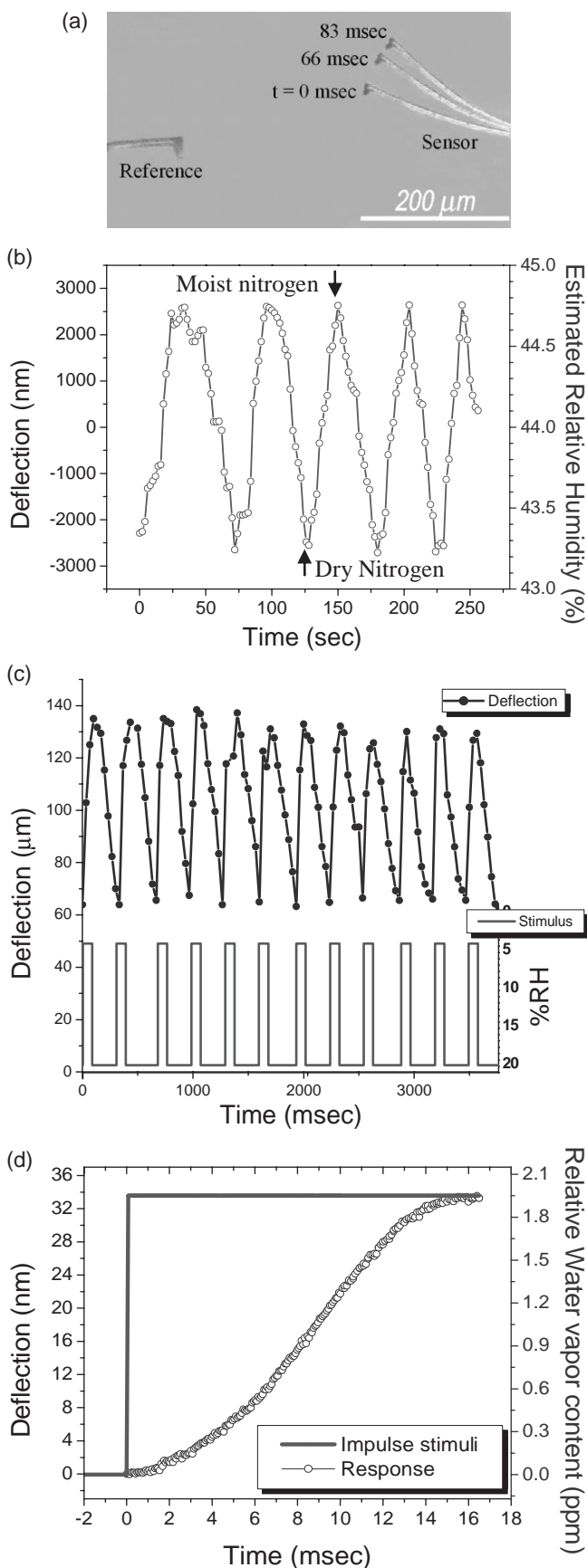
ADVANCED MATERIALS

Figure 22. Dynamic response of MC coated with ppMAN for repeated cycles of humidification and desiccation: a) Overlaid snap shots of the cantilevers depicting the response to nitrogen pulse b) Deflection of the cantilever under desiccating nitrogen pulses followed by relaxation to humid state. c) Response to cycles of small variations of humidity. d) Deflection of cantilever to a sudden change in humidity (0.01 % step) [237].

very stable, if no detonator is present. Their explosive power, however, is very large, and moreover, the vapor pressures of PETN and RDX are very low, in the range of ppb and ppt making them very difficult to detect.

Pinnaduwage et al. have reported the detection of 10 to 30 ppt of PETN and RDX using MCs functionalized with a SAM of 4-mercaptobenzoic acid.[128] The authors suggested that the hydrogen bonding between the nitro groups of the explosives molecule and the hydroxyl groups of the MBA is responsible for the reversible adsorption. The same group has demonstrated detection of DNT using SXFA-[poly(1-(4-hydroxy-4-trifluoromethyl-5,5,5-trifluoro)pent-1-enyl)methylsiloxane] polymer-coated MCs.[150] The nitro (NO_2) group on all of nitro aromatic explosives is highly electron deficient resulting in a high electron accepting ability for these molecules, which has been exploited for the specific recognition of the nitroaromatic explosives. In recent study, Tsukruk and co workers have also demonstrated a plasma polymerized benzonitrile coated MCs exhibited extremely high static deflection with a low detection limit below 10 ppb to hydrazine, a potentially explosive vapor.[237]

The second method involves a microexplosion of the molecules sticking to MC surface by an electrical pulse, which results in an exothermic spike in the static deflection signal of the MC as shown in Figure 23.[241] This spike was found to be related to the heat produced during deflagration. The amount of heat released is proportional to the area vs. bending signal plot of the process. The detection of TNT via deflagration was demonstrated by Pinnaduwage et al.[242] who used piezoresistive microcantilevers. It is worth noting that the inherent stickiness of the TNT molecules was exploited without any special functionalization as well. E.g., TNT was found to readily stick to Si surfaces.[244,245] Due to the small difference in the affinity between the two surfaces of the MC, finite deflection was observed before the voltage pulse (Fig. 23). TNT vapor was observed to adsorb on its surface resulting in a decrease of the resonance frequency. Application of an electrical pulse (10 V, 10 ms) to the piezoresistive cantilever resulted in deflagration of the TNT causing a bump in the cantilever bending. The deflagration was found to be complete, as the same resonance frequency as before the experiment was observed. The amount of TNT mass involved was determined to be 50 pg.

This technique applied to the detection of PETN and RDX displayed a much slower reaction kinetics.[241,243] Traces of DNT in TNT have also been used for detection of TNT, because it is the major impurity in production grade TNT because DNT is a decomposition product of TNT. The satura-
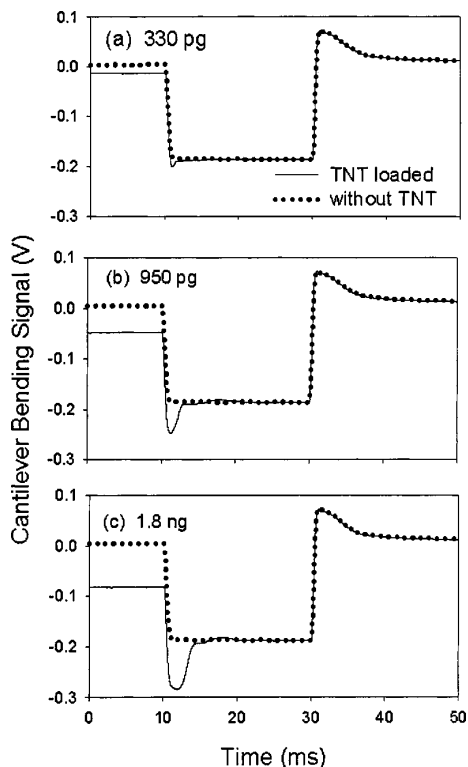
ADVANCED MATERIALS

Figure 23. Bending response of a MC in terms of voltage output from a position-sensitive detector to an applied voltage pulse with and without TNT adsorbed on the surfaces (a). Bending responses for loaded and unloaded situations are shown (b). The exothermic nature of the TNT deflagration event is clear due to the enhancement in bending of the cantilever. Reproduced with permission from [241]. Copyright 2004 American Institute of Physics.

tion concentration of DNT in air at 20 °C is 25 times higher than that of TNT. DNT was reported to be detected at the 300 ppt level using polysiloxane polymer layers.[150] Microfabrication of electrostatically actuated resonant microcantilevers in CMOS technology for detection of the nerve agent stimulant dimethylmethylphosphonate (DMMP) using polycarbosilane-coated MCs[246] is an important step towards an integrated platform, which besides compactness might also include telemetry.[247]

5. Mechanical Resonator Designs Beyond Single Cantilever Beams

5.1. Microcantilever Arrays

Single microcantilevers are prone to undesired external influences that may lead to additional bending. Influences may be, e.g., thermal drift or chemical interaction of a cantilever with its environment, in particular if the cantilever is operated in a liquid. Frequently, a baseline drift is observed during static measurements with unspecific physisorption of molecules on the cantilever surface or unspecific binding contributing to the drift.

To exclude such influences, simultaneous measurement of reference cantilevers without one-side modification is highly advantageous and is widely employed (Fig. 18).[101] From the difference in signals of reference and sensor cantilevers, the net cantilever response can be retrieved, and even small responses can be extracted from large cantilever deflections without being dominated by undesired effects. In contrast, for single microcantilevers, no thermal-drift compensation is possible. To obtain useful data under these circumstances, both microcantilever surfaces have to be chemically well-defined.

With a pair of cantilevers, reliable measurements can be usually obtained. One coated cantilever is used as the sensor cantilever, whereas the other cantilever serves as the reference one as discussed above. Thermal drifts are cancelled out by differential measurements, i.e., the difference in deflections is taken over the period of measurements. Alternatively, both cantilevers are used as sensor cantilevers (sensor layer on the upper surfaces), and the lower surface has to be passivated. The best strategy, however, is to use a cantilever array, in which several cantilevers are used either as sensors designated for different analytes or as reference cantilevers. In such a configuration, multiple difference signals can be evaluated simultaneously.

Several approaches exploiting integrated cantilever arrays are reported in literature. [110,226,248,249] An array of capacitively read-out micromachined cantilevers for measurement of adsorption-induced stress during exposure to hydrogen and mercury vapor was implemented as a handheld device including RF telemetry.[110] A polymer-coated complementary metal oxide semiconductor cantilever array for mass detection of volatile organic compounds in the dynamic mode has been tested with *n*-octane and toluene vapors.[226] Piezoresistive cantilever array coated with organic polymers have been reported to be capable of detecting methanol, 2-propanol, water and their binary mixtures to a wide range.[248] Two dimensional microcantilever arrays for multiplexed biomolecular analysis in liquids for DNA immobilization experiments have been successfully tested.[249]

5.2. Nanomechanical Resonators

While the thickness of typical MCs ranges from 0.5 to a few micrometers, the cantilevers with thickness below 100 nm can be fabricated and are termed as nanocantilevers (NCs). As the dimensions of the mechanical resonators shrink, the fundamental frequencies of these structures resemble the vibrational modes of molecules and atoms.[250] For a typical MC, the upper limit of the fundamental mode of the resonance frequency is on the order of 1 MHz. On the other hand, nanomechanical resonators can resonate at frequencies as high as 100 + MHz with a high quality factor, providing very high mass resolution reaching several attograms.[140,251]

Various materials such as metals, oxides, and ceramics have been applied for NC fabrication.[252–256] Nilsson et al have fabricated chromium NCs by e-beam lithography patterning of

ADVANCED MATERIALS

photoresist on a silicon substrate followed by the deposition of chromium and reactive ion etching to release the metal NCs.[253] Lavrik and Datskos reported the fabrication of NCs by FIB milling of MCs to alter the thickness of the MCs from 1.5 μm to 50–100 nm.[257] They reported the resonance frequency of 2.2 MHz and a very good mass resolution of 5.5 fg on chemisorption of 11-mercaptoundecanoic acid. Roukes et al have fabricated silicon carbide/metal NCs with embedded piezoresistors by epitaxially growing 70 nm thick cubic silicon carbide (3C SiC) coating followed by e-beam lithography and subsequent lift-off.[140,256] The NCs have been functionalized with 10 nm of PMMA for the detection of a trace level (1 ag at 127 MHz) of 1,1-difluoroethane.
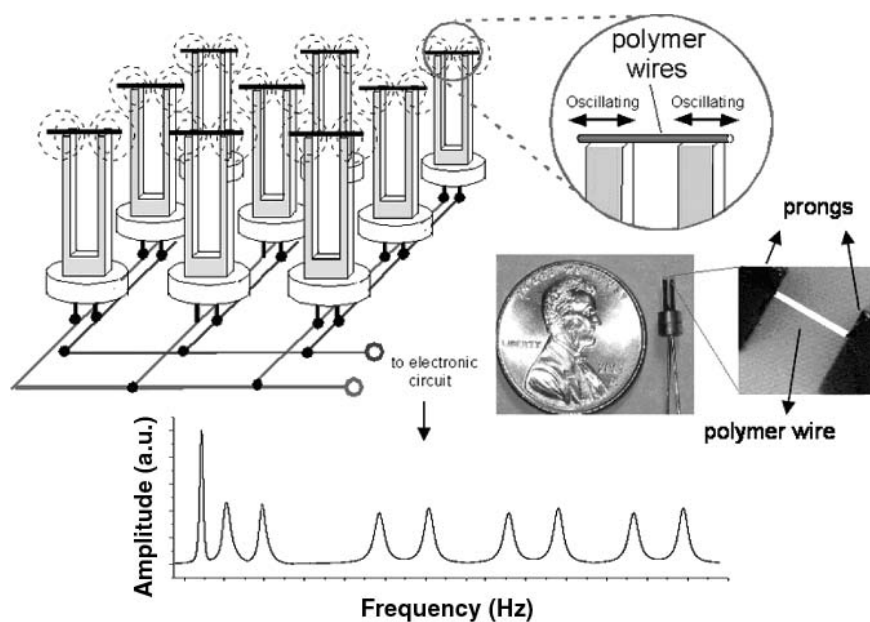

Figure 24. Array of tuning forks connected in the same electronic circuit with a polymer wire stretched across the prongs of each tuning fork and a spectrum of resonance responses. Reproduced with permission from [260]. Copyright 2005 American Chemical Society.

5.3. Tuning Fork Structures

Microfabricated tuning fork (MTF) structures (typical dimensions: 2 mm long, 200 μm wide, and 100 μm thick) similar to those traditionally used in wrist watches have been also been employed as tranducers for chemical sensors.[258] In the simplest form, tuning forks can be treated as two cantilevers coupled at the fixed end. The principle of opearation of TF based chemical sensors closely resembles that of the MC based sensors operating in dynamic mode where the external stimuli perturbs the resonating microstructures. One of the primary advantages of the tuning fork structures over MCs is the relatively high Q-factors (10^3–10^4) even under humid ambient conditions. Although the mass sensitivity of tuning fork devices is slightly lower, due to the high Q-factors, very small change (0.01 Hz) can be easily detected pushing mass resolution higher than that usually observed for regular cantilevers.

MTFs have been applied for chemical sensing, fluid viscosity measurements, specific biomolecule recognition and tactile sensing.[259–263] Zhang et al. have coated quartz tuning forks (with a resonance frequency of ∼ 33 KHz) with a thin PS layer from solution of varying concentration and showed a linear increase in the frequency shift with the mass attached on the tuning fork.[258] MTFs modified with anti-human IgG were applied to sense the binding of IgG within a range of 5–100 μg ml^{-1}.[263] Tao and coworkers have bridged a polymer nanowire (diameter of 100 nm) between the two arms of the MTFs by streching polymer gel (as shown in Fig. 24). They demonstrated that the resonance frequency of the MTF/polymer nanowire structure is related to the Young's modulus of the polymer structure by $E = \dfrac{2LK_{fork}}{Af_0}\Delta f_0$ where L and A are the length and the cross sectional area of the polymer wire,

K_{fork} is the effective spring constant, f_0 is the resonance frequency, and Δf_0 is the shift is the resonance frequency due to the presence of the polymer wire.[259] They have also shown reversible changes in the resonance frequency on exposure to organic vapors which can alter the elasticity of the polymer wire due to solvation effects. The technique has been further extended to achieve arrays of MTFs with different polymer wires to create a pattern of responses enabling the detection of various chemical vapors (water, ethylnitrobenzene, and ethanol vapors) with ppb level sensitivity.[260]

6. Conclusions and Outlook

In this review, we presented recent developments in the field of bimaterial cantilever sensors combined with different kinds of responsive coatings, mainly from soft materials. Responsive materials exploited for bimaterial MC designs are capable of selective swelling, binding, thermal expansion, chemical reactions, conformational changes, or decomposition under external stimuli. These stimuli lead to corresponding changes in interfacial stresses and thus cantilever bending facilitating facile detection of these stimuli hence sensing ability. Further development of novel responsive materials applied to MCs is desirable to provide multifunctional detection of a range of analytes a. k. a. an electronic nose. From a practical viewpoint, such materials should provide high compliance, strong adherance to the inorganic MC substrates, and the ability to mediate high interfacial stress. Nanoscale thickness of these responsive coatings is also a critical requirement which facilitates a fast response time, down to milisecond range from

ADVANCED MATERIALS

current second-minutes, a highly desirable characteristic demonstrated only in very few examples.

Apart from the numerous attractive attributes such as extreme sensitivity, versatility, excellent dynamic response, miniature size, and realiability, one of the primary reasons for the rapid progress of the bimaterial microcantilever-based technology is the commericial availability of the relatively inexpensive MCs and their arrays (initially deveoped for AFM) and available AFM optical detection system to quantify the MC bending with sub-nanometer precision. While the robust and sensitive AFM detection system suffices most of the requirements for the proof of principle stage, it is not the ideal choice for the real time application of the sensors. The limitations of the optical detection system, such as long equilibration time, consistent laser alignment, and thermal fluctuations can be largely minimized by applying piezoresistive, piezoelectric, and MOSFET methods. Moreover, the use of linear arrays allows with reference cantilevers increases the sensitivity of microcantilever measurements in both frequency and deflection modes.

From the numerous publications and laboratory scale demonstrations, it is obvious that MC based sensor technology has the efficacy to provide the next generation miniature, cost effective sensor arrays for a wide variety chemical and biological stimuli. However, for the technology to be transferred to real devices several important issues still need to be addressed in future studies. For example, a significant challenge for MC biosensor applications is the lack of quality reaction kinetics data that can be obtained, because the microcantilever are very sensitive to both changes in temperature and fluid flow. While smaller microcantilevers (nanocantilevers) may increase the sensitivity before and after addition of analyte, they also increase noise during analyte addition. Still better methods of detection need to be developed. It is clear that further improvements in microcantilever design and signal transduction will likely lead to the development of sensitive, selective and versatile detection devices for use in both gas and liquid environments. Commercialization of microcantilever array technology is already underway for complete detection of chemical, thermal, and biosensing.

Although the mass resolution and sensitivity of the nanocantilevers are highly attractive, significant efforts should be made in terms of developing reliable and economic methods for their large scale fabrication. The functionalization and readout methods are still serious challenges beyond the fabication of the NCs themselves. Conventional readout methods employed for MCs might not completely suffice the requirements due to various undesired effects such as parasitic capicitances and diffraction effects.

From the life sciences view point, MC sensor arrays are a very powerful and highly sensitive tool to study biochemical adsorption and desorption, complex biochemical reactions such as the hybridization of DNA, and molecular recognition in antibody/antigen systems. We believe that the development of the MC technology should go towards real-life applications, in particular practical assessment of clinical samples. The development of medical diagnosis tools requires further improvement of the sensitivity of a large number of genetic tests to be performed with small amount of single donor-blood or body-fluid samples at low cost. In a scientific perspective, the challenge lies in optimizing robust microcantilever sensors in such an extent that their sensitivity is improved to the ultimate limit, i.e., the detection of individual molecules.

[1] R. J. Colton, J. N. Russell, *Science* **2003**, *299*, 1324.
[2] M. Cabodi, S. W. P. Turner, H. G. Craighead, *Anal. Chem.* **2002**, *74*, 5169.
[3] D. S. Moore, *Sens. Imaging* **2007**, *8*, 9.
[4] I. Luzinov, S. Minko, V. V. Tsukruk, *Prog. Polym. Sci.* **2004**, *29*, 635.
[5] B. Zhao, W. J. Brittain, *Prog. Polym. Sci.* **2000**, *25*, 677.
[6] B. Adhikari, S. Majumdar, *Prog. Polym. Sci.* **2004**, *29*, 699.
[7] T. P. Russel, *Science* **2002**, *297*, 964.
[8] Y. Tezuka, H. Oike, *Prog. Polym. Sci.* **2002**, *27*, 1069.
[9] S. S. Sheiko, M. Moller, *Chem. Rev.* **2001**, *101*, 4099.
[10] D. A. Tomalia, J. M. Fréchet, *Prog. Polym. Sci.* **2005**, *30*, 217.
[11] Y. Lu, S. C. Chen, *Adv. Drug Delivery Rev.* **2004**, *56*, 1621.
[12] R. Langer, N. Peppas, *AIChE J.* **2003**, *49*, 2990.
[13] B. Jeong, A. Gutowska, *Trends Biotechnol.* **2002**, *20*, 305.
[14] S. Middelhoek, J. W. Noorlag, *Sens. Actuators* **1981/82**, *2*, 29.
[15] R. Mason, C. A. Jalbert, P. A. V. O'Rourke Muisener, J. T. Koberstein, J. F. Elman, T. E. Long, B. Z. Gunesin, *Adv. Colloid Interface Sci.* **2001**, *94*, 1.
[16] V. V. Tsukruk, *Prog. Polym. Sci.* **1997**, *22*, 247.
[17] C. Jiang, V. V. Tsukruk, *Adv. Mater.* **2006**, *18*, 829.
[18] E. S. Gil, S. M. Hudson, *Prog. Polym. Sci.* **2004**, *29*, 1173.
[19] *Responsive Polymer Materials* (Ed: S. Minko), Blackwell Publishing, Ames **2006**.
[20] R. Yerushalmi, A. Scherz, M. E. van der Boom, H.-B. Kraatz, *J. Mater. Chem.* **2005**, *15*, 4480.
[21] V. V. Tsukruk, V. N. Bliznyuk, *Prog. Polym. Sci.* **1997**, *22*, 1089.
[22] A. Ulman, *Chem. Rev.* **1996**, *96*, 1533.
[23] J. C. Love, L. A. Estroff, J. K. Kriebel, R. G. Nuzzo, G. M. Whitesides, *Chem. Rev.* **2005**, *105*, 1103.
[24] I. Luzinov, D. Julthongpiput, A. Liebmann-Vinson, T. Cregger, M. D. Foster, V. V. Tsukruk, *Langmuir* **2000**, *16*, 504.
[25] V. V. Tsukruk, *Adv. Mater.* **2001**, *13*, 95.
[26] C. H. Alarcon, S. Pennadam, C. Alexander, *Chem. Soc. Rev.* **2005**, *34*, 276.
[27] N. Nath, A. Chilkoti, *Adv. Mater.* **2002**, *14*, 1243.
[28] M. H. Nordby, A. Kjøniksen, B. Nystrom, J. Roots, *Biomacromolecules* **2003**, *4*, 337.
[29] B. Jeong, M. R. Kibbey, J. C. Birnbaum, Y. Won, A. Gutowska, *Macromolecules* **2000**, *33*, 8317.
[30] M. Yamato, M. Utsumi, A. Kushida, C. Konno, A. Kikuchi, T. Okano, *Tissue Eng.* **2001**, *7*, 473.
[31] F. J. Schmitt, C. Park, J. Simon, H. Ringsdorf, J. Israelachvili, *Langmuir* **1998**, *14*, 2838.
[32] M. E. Harmon, D. Kuckling, C. W. Frank, *Langmuir* **2003**, *19*, 10660.
[33] M. C. LeMieux, S. Peleshanko, K. D. Anderson, V. V. Tsukruk, *Langmuir* **2007**, *23*, 265.
[34] S. Peleshanko, K. D. Anderson, M. Goodman, M. D. Determan, S. K. Mallapragada, V. V. Tsukruk, *Langmuir* **2007**, *23*, 25.
[35] S. Y. Liu, S. P. Armes, *Langmuir* **2003**, *19*, 4432.
[36] S. Y. Liu, S. P. Armes, *Angew. Chem. Int. Ed.* **2002**, *41*, 1413.
[37] L. Ionov, S. Minko, M. Stamm, J.-F. Gohy, R. Jérôme, A. Scholl, *J. Am. Chem. Soc.* **2003**, *125*, 8302.

[38] Y. Liu, V. Klep, B. Zdyrko, I. Luzinov, *Langmuir* **2005**, *21*, 11806.

[39] R. Gunawidjaja, S. Peleshanko, V. V. Tsukruk, *Macromolecules* **2005**, *38*, 8765.

[40] L. Ionov, A. Sidorenko, M. Stamm, S. Minko, B. Zdyrko, V. Klep, I. Luzinov, *Macromolecules* **2004**, *37*, 7421.

[41] A. Kiriy, G. Gorodyska, S. Minko, C. Tsitsilianis, W. Jaeger, M. Stamm, *J. Am. Chem. Soc.* **2003**, *125*, 11202.

[42] R. C. Advincula, W. J. Brittain, K. C. Caster, J. Ruhe, *Polymer Brushes*, Wiley-VCH, Weinheim **2004**.

[43] S. Minko, *J. Macromol. Sci., Part C: Polym. Rev.* **2006**, *46*, 397.

[44] W. Brittain, S. J. Minko, *J. Polym. Sci. Part A* **2007**, *45*, 3505.

[45] J. Ruhe, M. Ballauff, M. Biesalski, P. Dziezok, F. Grohn, D. Johannsmann, N. Houbenov, N. Hugenberg, R. Konradi, S. Minko, M. Motornov, R. R. Netz, M. Schmidt, C. Seidel, M. Stamm, T. Stephan, D. Usov, H. N. Zhang, *Adv. Polym. Sci.* **2004**, *165*, 79.

[46] S. Santer, A. Kopyshev, J. Donges, H.-K. Yang, J. Rühe, *Macromolecules* **2006**, *39*, 3056.

[47] K. L. Genson, J. Holzmuller, O. F. Villacencio, D. V. McGrath, D. Vaknin, V. V. Tsukruk, *J. Phys. Chem. B* **2005**, *109*, 20393.

[48] D. Julthongpiput, Y.-H. Lin, J. Teng, E. R. Zubarev, V. V. Tsukruk, *Langmuir* **2003**, *19*, 7832.

[49] D. Julthongpiput, Y.-H. Lin, J. Teng, E. R. Zubarev, V. V. Tsukruk, *J. Am. Chem. Soc.* **2003**, *125*, 15912.

[50] Y.-H. Lin, J. Teng, E. R. Zubarev, H. Shulha, V. V. Tsukruk, *Nano Lett.* **2005**, *5*, 491.

[51] M. C. Lemieux, D. Julthongpiput, P. Duc Cuong, H.-S. Ahn, Y.-H. Lin, V. V. Tsukruk, *Langmuir* **2004**, *20*, 10046.

[52] M. Lemieux, D. Usov, S. Minko, M. Stamm, H. Shulha, V. V. Tsukruk, *Macromolecules* **2003**, *36*, 7244.

[53] D. T. McQuade, A. E. Pullen, T. M. Swager, *Chem. Rev.* **2000**, *100*, 2537.

[54] Z. Jin, Y. Su, Y. Duan, *Sens. Actuators B* **2000**, *71*, 118.

[55] J.-C. Chiang, A. G. MacDiarmind, *Synth. Met.* **1986**, *13*, 193.

[56] Y. Ito, Y. Ochiai, Y. S. Park, Y. Imanishi, *J. Am. Chem. Soc.* **1997**, *119*, 1619.

[57] H. Iwata, I. Hirata, Y. Ikada, *Macromolecules* **1998**, *31*, 3671.

[58] Y. Ito, S. Nishi, Y. S. Park, Y. Imanishi, *Macromolecules* **1997**, *30*, 5856.

[59] Y. S. Park, Y. Ito, Y. Imanishi, *Macromolecules* **1998**, *31*, 2606.

[60] Y. Sadaoka, Y. Sakai, H. Akiyama, *J. Mater. Sci.* **1986**, *21*, 235.

[61] C. K. Chian, Y. W. Park, A. J. Heeger, H. Shirakawa, E. J. Louis, A. G. MacDiarmid, *J. Chem. Phys.* **1978**, *69*, 5098.

[62] A. F. Diaz, K. K. Kanazawa, G. P. Gardini, *J. Chem. Soc. Chem. Commun.* **1979**, 635.

[63] J. Roncali, *Chem. Rev.* **1992**, *92*, 711.

[64] M. E. Nicho, M. Trejo, A. Garcia-Valenzuela, J. M. Saniger, J. Palacios, H. Hu, *Sens. Actuators B* **2001**, *77*, 657.

[65] G. Harsanyi, *Polymer Films in Sensor Applications*, Technomic, Lancaster **1995**.

[66] I. Tokareva, S. Minko, J. H. Fendler, E. Hutter, *J. Am. Chem. Soc.* **2004**, *126*, 15950.

[67] M. Motornov, R. Sheparovych, R. Lupitskyy, E. MacWilliams, S. Minko, *J. Colloid Interface Sci.* **2007**, *310*, 481.

[68] K. L. Genson, J. Holzmueller, C. Jiang, J. Xu, J. D. Gibson, E. R. Zubarev, V. V. Tsukruk, *Langmuir* **2006**, *22*, 7011.

[69] C. Jiang, H. Ko, V. V. Tsukruk, *Adv. Mater.* **2005**, *17*, 2127.

[70] C. Jiang, S. Markutsya, V. V. Tsukruk, *Langmuir* **2004**, *20*, 882.

[71] J. Li, H. Möhwald, Z. An, G. Lu, *Soft Matter* **2005**, *1*, 259.

[72] F. Caruso, *Adv. Mater.* **2001**, *13*, 11.

[73] C. Jiang, S. Markutsya, Y. Pikus, V. V. Tsukruk, *Nat. Mater.* **2004**, *3*, 721.

[74] X. Shi, M. Shen, H. Möhwald, *Prog. Polym. Sci.* **2004**, *29*, 987.

[75] H.-L. Zhang, S. D. Evans, J. R. Henderson, R. E. Miles, T.-H. Shen, *Nanotechnology* **2002**, *13*, 439.

[76] D. Li, Y. Jiang, Z. Wu, X. Chen, Y. Li, *Sens. Actuators B* **2000**, *66*, 125.

[77] A. F. Revzin, K. Sirkir, A. Simonian, M. V. Pishoko, *Sens. Actuators B* **2002**, *81*, 359.

[78] S. Myler, S. D. Collyer, K. A. Bridge, S. P. J. Higson, *Biosens. Bioelectron.* **2002**, *17*, 35.

[79] G. Binnig, C. F. Quate, C. Gerber, *Phys. Rev. Lett.* **1986**, *56*, 930.

[80] S. Karrasch, R. Hegerl, J. H. Hoh, W. Baumeister, A. Engel, *Proc. Natl. Acad. Sci. USA* **1994**, *91*, 836.

[81] D. J. Muller, F. A. Schabert, G. Buldt, A. Engel, *Biophys. J.* **1995**, *68*, 1681.

[82] J. K. Gimzewski, C. Gerber, E. Meyer, R. R. Schlittler, *Chem. Phys. Lett.* **1994**, *217*, 589.

[83] J. Hazel, V. V. Tsukruk, *J. Tribol.* **1998**, *120*, 814.

[84] J. L. Hazel, V. V. Tsukruk, *Thin Solid Films* **1999**, *339*, 249.

[85] G. G. Stoney, *Proc. R. Soc. London Ser. A* **1909**, *82*, 172.

[86] F. J. von Preissig, *J. Appl. Phys.* **1989**, *66*, 4262.

[87] C. A. Klein, *J. Appl. Phys.* **2000**, *88*, 5487.

[88] T. Thundat, R. J. Warmack, G. Y. Chen, D. P. Allison, *Appl. Phys. Lett.* **1994**, *64*, 2894.

[89] R. Berger, H. P. Lang, C. Gerber, J. K. Gimzewski, J. H. Fabian, L. Scandella, E. Meyer, H.-J. Güntherodt, *Chem. Phys. Lett.* **1998**, *294*, 363.

[90] T. Braun, V. Barwich, M. K. Ghatkesar, A. H. Bredekamp, C. Gerber, M. Hegner, H. P. Lang, *Phys. Rev. E* **2005**, *72*, 031907.

[91] T. P. Berg, M. Godin, S. M. Kundsen, W. Shem, G. Carlson, J. S. Foster, K. Babcock, S. R. Manalis, *Nature* **2007**, *446*, 1066.

[92] P. J. Shaver, *Rev. Sci. Instrum.* **1969**, *40*, 901.

[93] S. P. Timoshenko, *J. Opt. Soc. Am.* **1925**, *11*, 233.

[94] J. P. Cleveland, S. Manne, D. Bocek, P. K. Hansma, *Rev. Sci. Instrum.* **1993**, *64*, 403.

[95] T. Bachels, R. Schäfer, *Chem. Phys. Lett.* **1999**, *300*, 177.

[96] T. Bachels, F. Tiefenbacher, R. Schäfer, *J. Chem. Phys.* **1999**, *110*, 10008.

[97] S. Jeon, R. Desikan, F. Tian, T. Thundat, *Appl. Phys. Lett.* **2006**, *88*, 103118.

[98] G. Y. Chen, T. Thundat, E. A. Wachter, R. J. Warmack, *J. Appl. Phys.* **1995**, *77*, 3618.

[99] G. Meyer, N. M. Amer, *Appl. Phys. Lett.* **1988**, *53*, 1045.

[100] H.-P. Lang, M. Hegner, C. Gerber, *Mater. Today* **2005**, *8*, 30.

[101] H. P. Lang, R. Berger, C. Andreoli, J. Brugger, M. Despont, P. Vettiger, C. Gerber, J. K. Gimzewski, J.-P. Ramseyer, E. Meyer, H.-J. Güntherodt, *Appl. Phys. Lett.* **1998**, *72*, 383.

[102] H. J. Mamin, D. Rugar, *Appl. Phys. Lett.* **2001**, *79*, 3358.

[103] D. Rugar, H. J. Mamin, P. Guethner, *Appl. Phys. Lett.* **1989**, *55*, 2588.

[104] P. I. Oden, P. G. Datskos, T. Thundat, R. J. Warmack, *Appl. Phys. Lett.* **1996**, *69*, 3277.

[105] N. Abedinov, P. Grabiec, T. Gotszalk, T. Ivanov, J. Voigt, I. W. Rangelow, *J. Vac. Sci. Technol. A* **2001**, *19*, 2884.

[106] M. Tortonese, R. C. Barrett, C. F. Quate, *Appl. Phys. Lett.* **1996**, *62*, 834.

[107] Q. M. Wang, L. E. Cross, *Ferroelectrics* **1998**, *215*, 187.

[108] S. Zurn, M. Hseih, G. Smith, D. Markus, M. Zang, G. Hughes, Y. Nam, M. Arik, D. Polla, *Smart Mater. Struct.* **2001**, *10*, 252.

[109] J. D. Adams, B. Rogers, L. Manning, Z. Hu, T. Thundat, H. Cavazos, S. C. Minne, *Sens. Actuators A* **2005**, *121*, 457.

[110] C. L. Britton, R. L. Jones, P. I. Oden, Z. Hu, R. J. Warmack, S. F. Smith, W. L. Bryan, J. M. Rochelle, *Ultramicroscopy* **2000**, *82*, 17.

[111] R. Amantea, C. M. Knoedler, F. P. Pantuso, V. K. Patel, D. J. Sauer, J. R. Tower, *Proc. SPIE-Int. Soc. Opt. Eng.* **1997**, *3061*, 210.

[112] G. Shekawat, S.-H. Tark, V. P. Dravid, *Science* **2006**, *311*, 1592.

[113] M. Madou, *Fundamentals of Microfabrication*, CRC Press, New York **1997**.

[114] J. Buhler, F. P. Steiner, H. Baltes, *J. Micromech. Microeng.* **1997**, *7*, R1.

[115] A. Johansson, M. Calleja, P. A. Ramussen, A. Biosen, *Sens. Actuators B* **2005**, *123–124*, 111.

[116] M. Calleja, M. Nordstorm, M. Alvarez, J. Tamayo, L. M. Lechuga, A. Biosen, *Ultramicroscopy* **2005**, *105*, 215.

[117] A. W. McFarland, M. A. Poggi, L. A. Bottomley, J. S. Colton, *Nanotechnology* **2004**, *15*, 1628.

[118] A. W. McFarland, J. S. Colton, *J. Microelectromech. Syst.* **2005**, *14*, 1375.

[119] F. Hua, T. Cui, Y. M. Lvov, *Nano Lett.* **2004**, *4*, 823.

[120] T. Thundat, E. A. Wachter, S. L. Sharp, R. J. Warmack, *Appl. Phys. Lett.* **1995**, *66*, 1695.

[121] A. Boisen, J. Thaysen, H. Jensenius, O. Hansen, *Ultramicroscopy* **2000**, *11*, 82.

[122] Q. Zhao, Q. Zhu, W. Y. Shih, W.-H. Shih, *Sens. Actuators B* **2006**, *117*, 74.

[123] A. Kadam, G. P. Nordin, M. A. George, *J. Vac. Sci. Technol. B* **2006**, *24*, 2271.

[124] J. Mertens, M. Calleja, D. Ramos, A. Taryn, J. Tamayo, *J. Appl. Phys.* **2007**, *101*, 034904.

[125] D. Lee, E.-H Kim, M. Yoo, N. Jung, K. H. Lee, S. Jeon, *Appl. Phys. Lett.* **2007**, *90*, 113107.

[126] H.-F. Ji, E. Finot, R. Debestani, T. Thundat, G. M. Brown, P. F. Britt, *Chem. Commun.* **2000**, 457.

[127] H.-F. Ji, T. Thundat, R. Dabestani, G. M. Brown, P. F. Britt, P. V. Bonnesen, *Anal. Chem.* **2001**, *73*, 1572.

[128] L. A. Pinnaduwage, V. Boiadjiev, J. E. Hawk, T. Thudat, *Appl. Phys. Lett.* **2003**, *83*, 1471.

[129] Y. Yang, H. F. Ji, T. Thundat, *J. Am. Chem. Soc.* **2003**, *125*, 1124.

[130] P. Dutta, P. Chapman, P. G. Datskos, M. J. Sepaniak, *Anal. Chem.* **2005**, *77*, 6601.

[131] S.-H. S. Lim, D. Raorane, S. Satyanarayana, A. Majumdar, *Sens. Actuators B* **2006**, *119*, 466.

[132] G. Zuo, X. Li, P. Li, T. Yang, Y. Wang, Z. Cheng, S. Feng, *Anal. Chim. Acta* **2006**, *580*, 123.

[133] A. Bietsch, J. Zhang, M. Hegner, H. P. Lang, C. Gerber, *Nanotechnology* **2004**, *15*, 873.

[134] A. Bietsch, M. Hegner, H. P. Lang, C. Gerber, *Langmuir* **2004**, *20*, 5119.

[135] J. Amirola, A. Rodriguez, L. Casaner, J. P. Santos, J. Gutierrez, M. C. Horrillo, *Sens. Actuators B* **2005**, *111–112*, 247.

[136] D. Then, A. Vidic, C. Ziegler, *Sens. Actuators B* **2006**, *117*, 1.

[137] F. M. Battiston, J.-P. Ramseyer, H. P. Lang, M. K. Baller, C. Gerber, J. K. Gimzewski, E. Meyer, H.-J. Guntherodt, *Sens. Actuators B* **2001**, *77*, 122.

[138] B. H. Kim, F. E. Prins, D. P. Kern, S. Raible, U. Weimer, *Sens. Actuators B* **2001**, *78*, 12.

[139] T. A. Betts, C. A. Tipple, M. J. Sepaniak, P. G. Datskos, *Anal. Chim. Acta* **2000**, *422*, 89.

[140] M. Li, H. X. Tang, M. L. Roukes, *Nat. Nanotechnol.* **2007**, *2*, 114.

[141] M. K. Baller, H. P Lang, J. Fritz, C. Gerber, J. K. Gimzewski, U. Drechsler, H. Rothuizen, M. Despont, P. Vettinger, F. M. Battiston, J. P. Ramseyer, P. Fornaro, E. Meyer, H.-J. Guntherodt, *Ultramicroscopy* **2000**, *82*, 1.

[142] F. Lochon, L. Fadel, I. Dufour, D. Rebiere, J. Pistre, *Mater. Sci. Eng. C* **2006**, *26*, 348.

[143] J. Zhao, R. Berger, J. S. Gutmann, *Appl. Phys. Lett.* **2006**, *89*, 033110.

[144] M. C. LeMieux, M. E. McConney, Y. H. Lin, S. Singamaneni, H. Jiang, T. J. Bunning, V. V. Tsukruk, *Nano Lett.* **2006**, *6*, 730.

[145] Y. Zhang, H.-F. Ji, G. M. Brown, T. Thundat, *Anal. Chem.* **2003**, *75*, 4773.

[146] G.-G. Bumbu, G. Kircher, M. Wolkenhauer, R. Berger, J. S. Gutmann, *Macromol. Chem. Phys.* **2004**, *205*, 1713.

[147] N. I. Abu-Lail, M. Kaholek, B. LaMattina, R. L. Clark, S. Zauscher, *Sens. Actuators B* **2006**, *114*, 371.

[148] R. Bashir, J. Z. Hilt, O. Eilbol, A. Gupta, N. A. Peppas, *Appl. Phys. Lett.* **2002**, *81*, 3091.

[149] Y. H. Lin, M. E. McConney, M. C. LeMieux, S. Peleshanko, C. Jiang, S. Singamaneni, V. V. Tsukruk, *Adv. Mater.* **2006**, *18*, 1157.

[150] L. A. Pinnaduwage, T. Thundat, J. E. Hawk, D. L. Hedden, P. F. Britt, E. J. Houser, S. Stepnowski, R. A. McGill, D. Bubb, *Sens. Actuators B* **2004**, *99*, 223.

[151] T. Thundat, G. Y. Chen, R. J. Warmack, D. P. Allison, E. A. Wachter, *Anal. Chem.* **1995**, *67*, 519.

[152] H. Jiang, W. E. Johnson, J. T. Grant, K. Eyink, E. M. Johnson, D. W. Tomlin, T. J. Bunning, *Chem. Mater.* **2003**, *15*, 340.

[153] P. Tamirisa, K. C. Liddell, P. D. Pedrow, M. A. Osman, *J. Appl. Polym. Sci.* **2004**, *93*, 1317.

[154] H. Biederman, *Plasma Polymer Films*, Imperial College Press, London **2004**.

[155] D. Grbovic, N. V. Lavrik, P. G. Datskos, D. Forrai, E. Nelson, J. Devitt, B. McIntyre, *Appl. Phys. Lett.* **2006**, *89*, 073118.

[156] S. Singamaneni, M. LeMieux, H. Jiang, T. J. Bunning, V. V. Tsukruk, *Chem. Mater.* **2007**, *19*, 129.

[157] H. Biederman, Y. Osada, *Plasma Polymerization Processes*, Elsevier Science Publishers, Amsterdam, The Netherlands **1992**.

[158] J. W. Grate, *Chem. Rev.* **2000**, *100*, 2627.

[159] A. Hierlemann, A. J. Ricco, K. Bodenho, A. Dominik, W. GoÈpel, *Anal. Chem.* **2000**, *72*, 3696.

[160] J. W. Grate, S. J. Patrash, M. H. Abraham, *Anal. Chem.* **1995**, *67*, 2162.

[161] A. R. McGill, M. H. Abraham, J. W. Grate, *CHEMTECH* **1994**, *24*, 27.

[162] M. H. Abraham, J. Andonian-Haftvan, C. My Du, V. Diart, G. S. Whiting, J. W. Grate, R. A. McGill, *J. Chem. Soc. Perkin Trans.* **1995**, *2*, 369.

[163] J. W. Grate, M. H. Abraham, *Sens. Actuators B* **1991**, *3*, 85.

[164] M. Mao, T. Perazzo, O. Kwon, presented at the Microelectromechanical Systems, Nashville, TN, October 1999.

[165] P. G. Datskos, S. Rajic, L. R. Senesac, I. Datskou, *Ultramicroscopy* **2001**, *86*, 191.

[166] R. J. Kayes, *Optical and Infrared Detectors*, Springer, Berlin **1977**.

[167] J. L. Miller, *Principles of Infrared Technology*, Van Nostram Reinhold, New York **1994**.

[168] A. Rogalski, *Infrared Phys. Technol.* **1994**, *35*, 1.

[169] C. Hanson, *Infrared Technology XXI Proc. SPIE* **1993**, *2020*, 330.

[170] P. W. Kruse, in *Uncooled Infrared Imaging Arrays and Systems, Semiconductors and Semimetals*, Vol. 47 (Eds: P. W. Kruse, D. D. Skatrud), Academic Press, San Diego **1997**.

[171] P. W. Kruse, *Infrared Phys. Technol.* **1995**, *36*, 869.

[172] N. Butler, R. Blackwell, R. Murphy, R. Silva, C. Marshall, *Infrared Technology XXI, Proc. SPIE* **1995**, *2552*, 583.

[173] R. A. Wood, *Infrared Technology XXI, Proc. SPIE* **1993**, *2020*, 322.

[174] R.A. Wood, N. A. Foss, *Laser Focus World* **1993**, 101.

[175] P. G. Datskos, P. I. Oden, T. Thundat, E. A. Wachter, R. J. Warmack, S. R. Hunter, *Appl. Phys. Lett.* **1996**, *69*, 2986.

[176] P. I. Oden, E. A. Wachter, P. G. Datskos, T. Thundat, R. J. Warmack, *Infrared Technology XXII, Proc. SPIE* **1996**, *2744*, 345.

[177] T. Perazzo, M. Mao, O. Kwon, A. Majumdar, J. B. Varesi, P. Norton, *Appl. Phys. Lett.* **1999**, *74*, 3567.

[178] P. G. Datskos, S. Rajic, I. Datskou, *Appl. Phys. Lett.* **1998**, *73*, 2319.

[179] R. Amantea, C.M. Knoedler, F. P. Pantuso, presented at the Infrared Technology and Applications XXIII, Orlando, FL, March 1997.

[180] J. Lai, T. Perazzo, Z. Shi, A. Majumdar, *Sens. Actuators A* **1997**, *58*, 113.

[181] R. Amantea, L. A. Goodman, F. Pantuso, presented at the Infrared Technology and Applications XXIV, San Diego, CA, March 1998.

[182] L. R. Senesac, J. L. Corbeil, S. Rajic, N. V. Lavrik, P. G. Datskos, *Ultramicroscopy* **2003**, *97*, 451.

[183] E. A. Wachter, T. Thundat, P. I. Oden, R. J. Warmack, P. G. Datskos, S. L. Sharp, *Rev. Sci. Instrum.* **1996**, *67*, 3434.

[184] J. R. Barnes, R. J. Stephenson, M. E. Welland, C. Gerber, J. K. Gimzewski, *Nature* **1994**, *372*, 79.

[185] J. Varesi, J. Lai, T. Perazzo, Z. Shi, A. Majumdar, *Appl. Phys. Lett.* **1997**, *71*, 306.

[186] J. R. Barnes, R. J. Stephenson, C. N. Woodburn, S. J. O'Shea, M. E. Welland, T. Rayment, J. K. Gimzewski, C. Gerber, *Rev. Sci. Instrum.* **1994**, *65*, 3793.

[187] S. R. Manalis, S. C. Minne, C. F. Quate, G. G. Yaralioglu, A. Atalar, *Appl. Phys. Lett.* **1997**, *70*, 3311.

[188] J. L. Corbeil, N. V. Lavrik, S. Rajic, P. G. Datskos, *Appl. Phys. Lett.* **2002**, *81*, 1306.

[189] Y. Zhao, M. Mao, R. Horowitz, A. Majumdar, J. Varesi, P. Norton, J. Kitching, *J. MEMS* **2002**, *2*, 136.

[190] S. R. Hunter, R. A. Amantea, L. A. Goodman, D. B. Kharas, S. Gershtein, J. R. Matey, S. N. Perna, Y. Yu, N. Maley, L. K. White, *Proc. SPIE-Int. Soc. Opt. Eng.* **2003**, *5074*, 469.

[191] M. Godin, P. J. Williams, V. Tabard-Cossa, O. Laroche, L. Y. Beaulieu, R. B. Lennox, P. Grütter, *Langmuir* **2004**, *20*, 7090.

[192] R. Karlsson, A. Michaelsson, L. Mattsson, *J. Immunol. Meth.* **1991**, *145*, 229.

[193] K. Glasmastar, C. Larsson, F. Hook, B. Kasemo, *J. Colloid Interface Sci.* **2002**, *246*, 40.

[194] P. G. Ganesan, X. Wang, O. Nalamasu, *Appl. Phys. Lett.* **2006**, *89*, 213107.

[195] R. Berger, E. Delamarche, H. P. lang, C. Gerber, J. K. Gimzewski, E. Meyer, H.-J. Guntherodt, *Science* **1997**, *276*, 2021.

[196] S. Kohale, S. M. Molina, B. L. Weeks, R. Khare, L. J. Hope-Weeks, *Langmuir* **2007**, *23*, 1258.

[197] R. Zhang, K. Graf, R. Berger, *Appl. Phys. Lett.* **2006**, *89*, 223114.

[198] G.-G. Bumbu, M. Wolkenhauer, G. Kircher, J. S. Gutmann, R. Berger, *Langmuir* **2007**, *23*, 2203.

[199] S. Igarashi, A. N. Itakura, M. Toda, M. Kitajima, L. Chu, A. N. Chifen, R. Forch, R. Berger, *Sens. Actuators B* **2006**, *117*, 43.

[200] I. Pera, J. Fritz, *Langmuir* **2007**, *23*, 1543.

[201] A. M. Moulin, S. J. O'Shea, R. A. Bradley, P. Doyle, M. E. Welland, *Langmuir* **1999**, *15*, 8776.

[202] R. Mukhopadhyay, V. V. Sumbayev, M. Lorentzen, J. Kjems, P. Andreasen, F. Besenbacher, *Nano Lett.* **2005**, *5*, 2385.

[203] G. Wu, R.H. Datar, K. M. Hansen, T. Thundat, R. J. Cote, A. Majumdar, *Nat. Biotechnol.* **2001**, *19*, 856.

[204] A. Valiaev, N. I. Abu-Lail, D. W. Lim, A. Chilkoti, S. Zauscher, *Langmuir* **2007**, *23*, 339.

[205] J. Pei, F. Tian, T. Thundat, *Anal. Chem.* **2004**, *76*, 292.

[206] Y. Arntz, J. D. Seelig, H. P. Lang, J. Zhang, P. Hunziker, J. P. Ramseyer, E. Meyer, M. Hegner, C. Gerber, *Nanotechnology* **2003**, *14*, 86.

[207] N. Backmann, C. Zahnd, F. Huber, A. Bietsch, A. Pluckthun, H.-P. Lang, H.-J. Guntherodt, M. Hegner, C. Gerber, *Proc. Natl. Acad. Sci. USA* **2005**, *102*, 14587.

[208] Y. Lam, N. I. Abu-Lail, S. M. Alam, S. Zauscher, *Nanomedicine* **2006**, *2*, 222.

[209] C. Milburn, J. Zhou, O. Bravo, C. Kumar, W. O. Soboyejo, *J. Biomed. Nanotechnol.* **2005**, *1*, 30.

[210] L. A. Pinnaduwage, J. E. Hawk, V. Boiadjiev, D. Yi, T. Thundat, *Langmuir* **2003**, *19*, 7841.

[211] R. Raiteri, G. Nelles, H.-J. Butt, W. Knoll, P. Skladal, *Sens. Actuators B* **1999**, *61*, 213.

[212] C. A. Savran, S. M. Knudsen, A. D. Ellington, S. R. Manalis, *Anal. Chem.* **2004**, *76*, 3194.

[213] G. Wu, H. Ji, K. M. Hansen, T. Thundat, R. Datar, R. Cote, M. F. Hagan, A. Chakraborty, A. Majumdar, *Proc. Natl. Acad. Sci. USA* **2001**, *98*, 1560.

[214] J. Fritz, M. K. Baller, H.-P. Lang, H. Rothuizen, P. Vettiger, E. Meyer, H.-J. Guntherodt, C. Gerber, J. K. Gimzewski, *Science* **2000**, *288*, 316.

[215] K. M. Hansen, H.-F. Ji, G. Wu, R. Dater, R. Cote, A. Majumdar, T. Thundat, *Anal. Chem.* **2001**, *73*, 1567.

[216] R. McKendry, J. Zhang, Y. Arntz, T. Strunz, M. Hegner, H.-P. Lang, M. K. Baller, U. Certa, E. Meyer, H.-J. Guntherodt, C. Gerber, *Proc. Natl. Acad. Sci. USA* **2002**, *99*, 9783.

[217] K. Y. Gfeller, N. Nugaeva, M. Hegner, *Appl. Environ. Microbiol.* **2005**, *71*, 2626.

[218] A. Gupta, D. Akin, R. Bashir, *Appl. Phys. Lett.* **2004**, *84*, 1976.

[219] N. Nugaeva, K. Y. Gfeller, N. Backmann, H.-P. Lang, M. Duggelin, M. Hegner, *Biosens. Bioelectron.* **2005**, *21*, 849.

[220] T. Braun, N. Backmann, M. Vogtli, A. Bietsch, A. Engle, H.-P. Lang, C. Gerber, M. Hegner, *Biophys. J.* **2006**, *90*, 2970.

[221] H. P. Lang, M. K. Baller, R. Berger, C. Gerber, J. K. Gimzewski, F. M. Battiston, P. Fornaro, J. P. Ramseyer, E. Meyer, H.-J. Güntherodt, *Anal. Chim. Acta* **1999**, *393*, 59.

[222] S. Okuyama, Y. Mitobe, K. Okuyama, K. Matsushita, *Jpn. J. Appl. Phys., Part 1* **2000**, *39*, 3584.

[223] P. G. Datskos, M. J. Sepaniak, C. A. Tipple, N. Lavrik, *Sens. Actuators B* **2001**, *76*, 393.

[224] P. G. Datskos, S. Rajic, M. J. Sepaniak, N. Lavrik, C. A. Tipple, L. R. Senesac, I. Datskou, *J. Vac. Sci. Technol. B* **2001**, *19*, 1173.

[225] I. W. Rangelow, P. Grabiec, T. Gotszalk, K. Edinger, *Surf. Interface Anal.* **2002**, *33*, 59.

[226] D. Lange, C. Hagleitner, A. Hierlemann, O. Brand, H. Baltes, *Anal. Chem.* **2002**, *74*, 3084.

[227] K. Henkel, D. Schmeisser, *Anal. Bioanal. Chem.* **2002**, *374*, 329.

[228] P. A. Arutyunov, A. L. Tolstikhina, *Meas. Techniques* **2002**, *45*, 714.

[229] J. Zhou, P. Li, S. Zhang, Y. C. Long, F. Zhou, Y. P. Huang, P. Y. Yang, M. H. Bao, *Sens. Actuators B* **2003**, *94*, 337

[230] R. L. Gunter, W. G. Delinger, K. Manygoats, A. Kooser, T. L. Porter, *Sens. Actuators A* **2003**, *107*, 219.

[231] A. Kooser, K. Manygoats, M. P. Eastman, T. L. Porter, *Biosens. Bioelectron.* **2003**, *19*, 503.

[232] A. Kooser, R. L. Gunter, W. D. Delinger, T. L. Porter, M. P. Eastman, *Sens. Actuators B* **2003**, *99*, 474.

[233] Y. J. Wright, A. K. Kar, Y. W. Kim, C. Scholz, M. A George, *Sens. Actuators B* **2005**, *107*, 242.

[234] P. Dutta, L. R. Senesac, N. V. Lavrik, P. G. Datskos, M. J. Sepaniak, *Sens. Lett.* **2004**, *2*, 238.

[235] L. R. Senesac, P. Dutta, P. G. Datskos, M. J. Sepaniak, *Anal. Chim. Acta* **2006**, *558*, 94.

[236] R. Archibald, P. Datskos, G. Devault, V. Lamberti, N. Lavrik, D. Noid, M. Sepaniak, P. Dutta, *Anal. Chim. Acta* **2007**, *584*, 101.

[237] S. Singamaneni, M. McConney, M. C. LeMieux, H. Jiang, J. Enlow, R. Naik, T. J. Bunning, V. V. Tsukruk, *Adv. Mater.* **2007**, *19*, 4248.

[238] R. G. Ewing, C. J. Miller, *Field Anal. Chem. Technol.* **2001**, *5*, 215.

[239] A. N. Garroway, M. L. Buess, J. B. Miller, B. H. Suits, A. D. Hibbs, G. A. Barrall, R. Matthews, L. J. Burnett, *IEEE Trans. Geosci. Remote Sens.* **2001**, *39*, 1108.

[240] P. G. Datskos, N. V. Lavrik, M. J. Sepaniak, *Sens. Lett.* **2003**, *1*, 25.

[241] L. A. Pinnaduwage, A. Gehl, D. L. Hedden, G. Muralidharan, T. Thundat, R. T. Lareau, T. Sulchek, L. Manning, B. Rogers, M. Jones, J. D. Adams, *Nature* **2003**, *425*, 474.

[242] L. A. Pinnaduwage, A. Wig, D. L. Hedden, A. Gehl, D. Yi, T. Thundat, *J. Appl. Phys.* **2004**, *95*, 5871.

[243] L. A. Pinnaduwage, T. Thundat, A. Gehl, S. D. Wilson, D. L. Hedden, R. T. Lareau, *Ultramicroscopy* **2004**, *100*, 211.

[244] G. Muralidharan, A. Wig, L. A. Pinnaduwage, D. Hedden, T. Thundat, R. T. Lareau, *Ultramicroscopy* **2003**, *97*, 433.

[245] L. A. Pinnaduwage, D. Yi, F. Tian, T. Thundat, R. T. Lareau, *Langmuir* **2004**, *20*, 2690.

[246] I. Voiculescu, M. E. Zaghloul, R. A. McGill, E. J. Houser, G. K. Fedder, *IEEE Sens. J.* **2005**, *5*, 641.

[247] L. A. Pinnaduwage, H. F. Ji, T. Thundat, *IEEE Sens. J.* **2005**, *5*, 774.

[248] N. Abedinov, C. Popov, Z. Yordanov, T. Ivanov, T. Gotszalk, P. Grabiec, W. Kulisch, I. W. Rangelow, D. Filenko, Y. Shirshov, *J. Vac. Sci. Technol. B* **2003**, *21*, 2931.

[249] M. Yue, H. Lin, D.E. Dedrick, S. Satyanarayana, A. Majumdar, A. S. Bedekar, J. W. Jenkins, S. Sundaram, *J. Microelectromech. Syst.* **2004**, *13*, 290.

[250] A. N. Clelenad, M. L. Roukes, *J. Appl. Phys.* **2002**, *92*, 2758.

[251] Y. T. Yang, C. Callagari, X. L. Ekinci, M. L. Roukes, *Nano Lett.* **2006**, *6*, 583.

[252] Z. J. Davis, A. Boisen, *Appl. Phys. Lett.* **2005**, *87*, 013102.

[253] S. G. Nilsson, E.-L. Sarwe, L. Montelius, *Appl. Phys. Lett.* **2003**, *83*, 990.

[254] W. L. Hughes, Z. L. Wang, *Appl. Phys. Lett.* **2003**, *82*, 2886.

[255] Z. L. Wang, X. Y. Kong, J. M. Zuo, *Phys. Rev. Lett.* **2003**, *91*, 185502.

[256] Y. T. Yang, K. L. Ekinci, X. M. H. Huang, L. M. Schiavone, M. L. Roukes, C. A. Zorman, M. Mehregany, *Appl. Phys. Lett.* **2001**, *78*, 162.

[257] N. V. Lavrik, P. G. Datskos, *Appl. Phys. Lett.* **2003**, *82*, 2697.

[258] J. Zhang, S. O'Shea, *Sens. Actuators B* **2003**, *94*, 65.

[259] S. Boussaad, N. J. Tao, *Nano Lett.* **2003**, *3*, 1173.

[260] M. Ren, E. S. Forzani, N. Tao, *Anal. Chem.* **2003**, *77*, 2700.

[261] H. Itoh, Y. Yamada, *Jpn. J. Appl. Phys., Part 1* **2006**, *45*, 4643.

[262] A. A. Kosterev, F. K. Tittel, D. V. Serebryakov, A. L. Malinovsky, I. V. Morozov, *Rev. Sci. Instr.* **2005**, *76*, 043105.

[263] X. Su, C. Dai, J. Zhang, S. J. O'Shea, *Biosens. Bioelec.* **2002**, *17*, 111.